











**ORIGINAL RESEARCH**

# The Protective Role of Yin-Yang 1 in Cardiac Injury and Remodeling After Myocardial Infarction

Yu Huang , MD\*; Liangpeng Li, MD\*; Hongmei Chen , MD\*; Qiao Liao , MS\*; Xiaoli Yang , MD; Dezhong Yang , MD; Xuwei Xia , MS; Hongyong Wang , MD; Wei Eric Wang , MD, PhD; Lianglong Chen , MD, PhD; Chunyu Zeng , MD, PhD

**BACKGROUND:** Exploring potential therapeutic target is of great significance for myocardial infarction (MI) and post-MI heart failure. Transcription factor Yin-Yang 1 (YY1) is an essential regulator of apoptosis and angiogenesis, but its role in MI is unclear.

**METHODS AND RESULTS:** The expression of YY1 was assessed in the C57BL/6J mouse heart following MI. Overexpression or silencing of YY1 in the mouse heart was achieved by adeno-associated virus 9 injection. The survival, cardiac function, and scar size, as well as the apoptosis, angiogenesis, cardiac fibrosis, T helper 2 lymphocyte cytokine production, and macrophage polarization were assessed. The effects of YY1 on Akt phosphorylation and vascular endothelial growth factor production were also investigated. The expression of YY1 in heart was significantly stimulated by MI. The survival rate, cardiac function, scar size, and left ventricular volume of mice were improved by YY1 overexpression but worsened by YY1 silencing. YY1 alleviated cardiac apoptosis and fibrosis, promoted angiogenesis, T helper 2 cytokine production, and M2 macrophage polarization in the post-MI heart, it also enhanced the tube formation and migration ability of endothelial cells. Enhanced Akt phosphorylation, along with the increased vascular endothelial growth factor levels were observed in presence of YY1 overexpression.

**CONCLUSIONS:** YY1 ameliorates cardiac injury and remodeling after MI by repressing cardiomyocyte apoptosis and boosting angiogenesis, which might be ascribed to the enhancement of Akt phosphorylation and the subsequent vascular endothelial growth factor up-regulation. Increased T helper 2 cytokine production and M2 macrophage polarization may also be involved in YY1's cardioprotective effects. These findings supported YY1 as a potential target for therapeutic investigation of MI.

**Key Words:** angiogenesis ■ apoptosis ■ myocardial infarction ■ vascular endothelial growth factor ■ YY1

**M**yocardial infarction (MI) is a leading cause of death worldwide.<sup>1</sup> Exploring potential therapeutic targets is of great significance. Pathological processes such as apoptosis, angiogenesis, and fibrosis play an essential role in MI and cardiac remodeling<sup>2</sup>; however, the underlying mechanism remains not fully understood.

Yin-Yang1 (YY1) is a ubiquitous and multifunctional zinc-finger transcription factor and belongs to the polycomb group protein family. YY1 regulates a variety of genes that are implicated in cell cycle, apoptosis, and angiogenesis.<sup>3</sup> YY1 has been shown to participate in the development of cancer.<sup>4</sup> The increased levels of YY1 expression were observed in human failing hearts

Correspondence to: Chunyu Zeng, MD, PhD, Department of Cardiology, Daping Hospital, Third Military Medical University, No. 10 Chang-Jiang Brunch Road, Chongqing 400042, P. R. China. E-mail: chunyuzeng01@163.com and Lianglong Chen, MD, PhD, Department of Cardiology, Fujian Heart Medical Center, Fujian Institute of Coronary Heart Disease, Fujian Medical University Union Hospital, No. 29 Xin-Quan Road, Fuzhou 350001, Fujian, P. R. China. E-mail: lianglongchen@126.com

\*Y. Huang, L. Li, H. Chen, and Q. Liao contributed equally.

Supplementary Material for this article is available at <https://www.ahajournals.org/doi/suppl/10.1161/JAHA.121.021895>

For Sources of Funding and Disclosures, see page 11.

© 2021 The Authors. Published on behalf of the American Heart Association, Inc., by Wiley. This is an open access article under the terms of the Creative Commons Attribution-NonCommercial-NoDerivs License, which permits use and distribution in any medium, provided the original work is properly cited, the use is non-commercial and no modifications or adaptations are made.

JAHA is available at: [www.ahajournals.org/journal/jaha](http://www.ahajournals.org/journal/jaha)

## CLINICAL PERSPECTIVE

### What Is New?

- The role of the transcription factor Yin-Yang 1 in myocardial infarction (MI) is unclear, we found that the expression of Yin-Yang 1 is induced in mouse heart after MI, and that Yin-Yang 1 increases angiogenesis, represses cardiac apoptosis, and ameliorates cardiac remodeling after MI by enhancing Akt phosphorylation and the subsequent VEGF production.

### What Are the Clinical Implications?

- Cardiomyocyte apoptosis and angiogenesis are 2 important events after MI, our study may provide experimental basis for exploring Yin-Yang 1 as a potential therapeutic target for cardiac remodeling after MI.

## Nonstandard Abbreviations and Acronyms

<b>AAV9</b>	adeno-associated virus 9
<b>NRVM</b>	neonatal rat ventricular myocytes
<b>shYY1</b>	short hairpinYY1
<b>Th2</b>	T helper 2
<b>YY1</b>	Yin-Yang 1

and were thought to play a role in suppressing the alpha myosin heavy chain promoter,<sup>5</sup> which is detrimental to heart function. On the other hand, the same group showed that YY1 protected cardiomyocytes from pathological hypertrophy via functional association with histone deacetylase 5.<sup>6</sup> However, whether or not YY1 plays a role in MI remains unclear.

In the present study, we investigated the expression of YY1 in the mouse heart following MI and explored whether and how YY1 affects MI injury and cardiac remodeling.

## METHODS

The data that support the findings of this study are available from the corresponding author upon reasonable request.

### Production of Adeno-Associated Virus 9-YY1 and Adeno-Associated Virus 9-Short Hairpin RNA Against YY1

Recombined adeno-associated virus 9 (AAV9)-YY1 (Obio, Shanghai, China) is produced in human 293T cells with insertion of YY1 cDNA sequence into AAV9

vector. YY1 cDNA was firstly amplified with primers and fused into the pAAV-CAG-EGFP vector with seamless-cloning method and sequenced. Then the engineered vector was cotransfected with pHelper and pRC (for AAV9 rep and cap expression) plasmid to 293T cells for viral production. After 72-hour incubation, cells were harvested and disrupted. Recombined AAV9 particles were isolated with the freeze-thaw method and purified by cesium chloride concentration gradient centrifugation for 48 hours, with 2 rounds. Virus was tittered with a quantitative polymerase chain reaction (PCR) test to Woodchuck hepatitis virus posttranscriptional regulatory element sequence and stocked at  $-80^{\circ}\text{C}$ . AAV9 for empty pAAV-CAG6-EGFP vector sequence was used as the control in the experiments.

Recombined AAV9-short hairpinYY1 is produced by insertion of short hairpin RNA for YY1 sequence targeting mouse YY1 mRNA (5'-CGACGGTTGTAATAAGAAGTT-3') into the pAAV-U6-spgRNA v2.0 [short hairpin RNA]-CMV-EGFP-Woodchuck hepatitis virus posttranscriptional regulatory element -spolyA vector. Insertion of the validated negative control sequence (5'-CCTAAGGTTAAGTCGCCCTCG-3') into the vector served as scramble control (AAV9-scramble). The viral production procedure is similar to that of AAV9-YY1.

### MI Model and Intramyocardial Delivery of AAV9

Male C57BL/6J mice aged 8 weeks old (Purchased from Shanghai Model Organisms, China) were randomized and assigned to groups. The mice were anesthetized with isoflurane inhalation. Artificial respiration was maintained with a rodent ventilator (Harvard Apparatus, Holliston, MA). The heart was exposed upon opening the left pleural cavity by cutting the intercostal muscles between left third and fourth ribs. The pericardium was removed, and left anterior descending coronary artery was occluded 2 to 3 mm from its origin with a 7-0 silk suture. The immediate death (within 24 hours) after the operation, and the mice with normal cardiac function 1 week after MI would be excluded from the experiment. Two of 21 in the AAV9-GFP group, 1 of 19 in the AAV9-YY1 group, 2 of 20 in the AAV9-scramble group, and 3 of 21 in the AAV9-shYY1 group were excluded according to the criteria.

As for virus administration, a syringe fitted with a 29-G needle was inserted near the border of the ischemic zone at the 5 point and tunneled intramuscularly to the anterior left ventricular wall. After slowly injecting total of 15  $\mu\text{L}$  of AAV particles ( $5 \times 10^{10}$  vg), the chest was closed in layers and a total of 0.1 mL 0.5% bupivacaine was injected subcutaneously near both edges of the skin incision to alleviate postoperative pain. The operation was performed blindly. All work was performed

under animal protocols approved by the Animal Care and Use Committee of the Third Military Medical University and conformed to the Guide for the Care and Use of Laboratory Animals (National Institutes of Health Publication 85–23, revised 1985).

### Echocardiography Analysis

Echocardiography was performed with GE Vivid E9 ultrasound machine (GE Healthcare, Chicago, IL) to determine the structure and function of the mouse heart. Ejection fraction was automatically calculated by the echocardiography software according to the Teicholz formula. Parameters including diastolic left ventricular internal diameter were measured to determine structural changes in cardiac morphology. The individuals conducting the experiment were blinded to the animal treatments.

### Infarct Size Determination

Similar to previous description,<sup>7</sup> the mouse heart (4 weeks after MI) was cut as 4- $\mu$ m-thick sections. Masson's trichrome staining was performed with Masson's trichrome kit (Solarbio, Beijing, China) according to the instruction. The percentage of fibrotic area of the left ventricle was measured using Image J software (National Institutes of Health, Bethesda, MD). Digital images were captured and infarct sizes were calculated according to the formula: [infarct perimeter (epicardial+endocardial)/total perimeter (epicardial+endocardial)] $\times$ 100. Individuals conducting the experiment were blinded to the experimental groups.

### Isolation, Culturing, and Treatment of Neonatal Rat Ventricular Myocytes

The isolation and culturing of neonatal rat ventricular myocytes (NRVMs) were performed as described previously in detail.<sup>7</sup> The hearts of 1- to 2-day-old Sprague-Dawley rats were minced, and the cardiomyocytes were dissociated with 1.5 mg/mL trypsin (Gibco, NY), collected and plated in fibronectin (10  $\mu$ g/mL) coated Millicell EZ slides (Millipore, Burlington, MA) for immunostaining. Cells were placed in an atmosphere composed of 1% O<sub>2</sub>, 5% CO<sub>2</sub>, and 94% N<sub>2</sub> to mimic the hypoxic condition in a trigas incubator (Thermo, CA). MK2206 were purchased from Selleck (Selleck, Shanghai, China), dissolved in DMSO and added to NRVMs at a final concentration of 3  $\mu$ mol/L 1 day after plasmid transfection.

### Histology and Immunostaining

Formalin fixed hearts were embedded in paraffin and cut as 4- $\mu$ m-thick sections. Anti-cardiac troponin I mouse antibody (cat#MA1-22700, Invitrogen, Waltham, MA), anti-CD31 rabbit antibody (cat#ab182981,

Abcam, Cambridge, UK), and 2-(4-Amidinophenyl)-6-indolecarbamide dihydrochloride (DAPI; Beyotime, Suzhou, China) were used to label cardiac troponin I, CD31, and nucleus, respectively. The terminal deoxynucleotidyl transferase mediated dUTP-biotin nick end labeling assay was conducted with in situ apoptotic cell death detection kit (Roche, Basel, Switzerland). The number of capillaries and apoptosis was counted in 5 random fields per section of the peri-infarct zone, and a total of 5 sections per animal were analyzed (N=5 for each group). Alexa Fluor 488- or Alexa Fluor 546-conjugated secondary antibodies (cat#A-21202, cat#A10040, Invitrogen) were applied appropriately to detect the primary antibodies. All the manual counts were performed in a blinded fashion. Cardiac fibrosis was quantitated by measuring the blue area in the Masson's trichrome-stained heart sections.

### Western Blot

The equal amount of proteins were separated by SDS-PAGE and transferred electrophoretically to polyvinylidene fluoride membranes (Bio-Rad Laboratories, Hercules, CA). The membranes were probed with YY1 antibody (cat#sc-7341, Santa Cruz, TX), Akt antibody (cat#4685, CST, MA), phosphorylated Akt (Serine 473) antibody (cat#5012, CST), cleaved caspase 3 antibody (cat#9664, CST), pan-caspase 3 antibody (cat#9662, CST, MA), VEGF A antibody (cat#66828-1-Ig, Proteintech, Wuhan, China) and  $\beta$ -actin antibody (cat#ZRB1312, Sigma, MA). The membrane signal was detected by appropriate secondary antibody (cat#926-68072, cat#925-32213, LI-COR Biosciences, Lincoln, NE), and then scanned with Odyssey CLX Imager system (LI-COR Biosciences). The densitometry values were normalized with  $\beta$ -actin protein signal.

### Real-Time PCR

For real-time PCR, total RNA was extracted from tissue or cells with TRIzol (Invitrogen) and purified with RNeasy kit (Qiagen, Hilden, Germany). Real-time PCR was performed using the brilliant SYBR green master mix kit and the CFX96 multiplex quantitative PCR System (Bio-Rad Laboratories). PCR primers (Sangon, Shanghai, China) are as follows: mouse YY1: sense primer: 5'-CAGAA GCAGGTGCAGATCAGACCCT-3', antisense primer: 5'-GCACCACCACCCACGGAATCG-3'; mouse  $\beta$ -actin: sense primer: 5'-GTTGGAGCAAACATCCCCCA-3', antisense primer: 5'-ACGCGACCATCCTCCTCTTA-3'.

### Plasmid and Cell Transfection

The YY1 overexpression plasmid (pcDNA3.1-YY1), and the short hairpin RNA against YY1 expression plasmid (pcENTRrhU6-shYY1), were previously reported<sup>4</sup> and kindly provided by Prof. Shourong Wu (College

of Bioengineering, Chongqing University, China). Cell transfection was performed with lipofectamine 3000 (Invitrogen), according to manufacturer's instruction.

### In Vitro Angiogenesis Assay

Capillary-like endothelial tube formation was evaluated by an in vitro angiogenesis assay. One hundred thirty microliters of matrigel basement membrane-matrix (BD Biosciences, San Jose, CA) was added to each well of precooled 24-well tissue culture plates. Pipette tips and matrigel solution were kept cold during the procedure to avoid solidification. The plates were incubated for 1 hour at 37 °C to allow matrix solution to solidify;  $4 \times 10^4$  human umbilical vein endothelial cells transfected with pcDNA 3.1 or pcDNA 3.1-YY1 in a final volume of 500  $\mu$ L endothelial cell basal medium-2 (Gibco) +2% fetal bovine serum (Gibco) were seeded in each matrix-coated well. Cells were stimulated with 100 ng/mL VEGF-A (Gibco) for 4 to 6 hours at 37 °C. The closed polygons formed in at least 6 random view microscopic fields per well were counted and values averaged.

### ELISA for VEGF-A

The levels of VEGF-A in the myocardium or serum were determined by ELISA using commercially available mouse VEGF-A Quantikine ELISA Kit (R&D Systems, Minneapolis, MN) according to the manufacturer's

instruction. The absorbance was subsequently measured on a spectrophotometer (Thermo).

### Statistical Analysis

Statistical analyses were performed by 1-way ANOVA followed by Bonferroni's multiple comparison test (for comparison of >2 groups) or Student *t* test (for comparison of 2 groups) (Prism 8.0, GraphPad Software Inc, La Jolla, CA). Data are given as mean $\pm$ SD, and a *P* value (2-sided) of <0.05 was considered significant. The log-rank test was used to compare survival curves.

The supplemental methods can be found in Data S1.

## RESULTS

### Expression of YY1 in Heart Was Elevated by MI

It has been reported the increased expression of YY1 in failing heart, but the expression of YY1 in heart following MI remains unclear. We found that in the C57BL/6J mouse heart, the protein expression of YY1 was increased after MI and lasted for weeks (Figure 1A). To investigate whether the induction of YY1 occurs in cardiomyocytes, we tested the YY1 expression in cultured cardiomyocytes (NRVMs) under hypoxia. Consistent with the in vivo experiments,

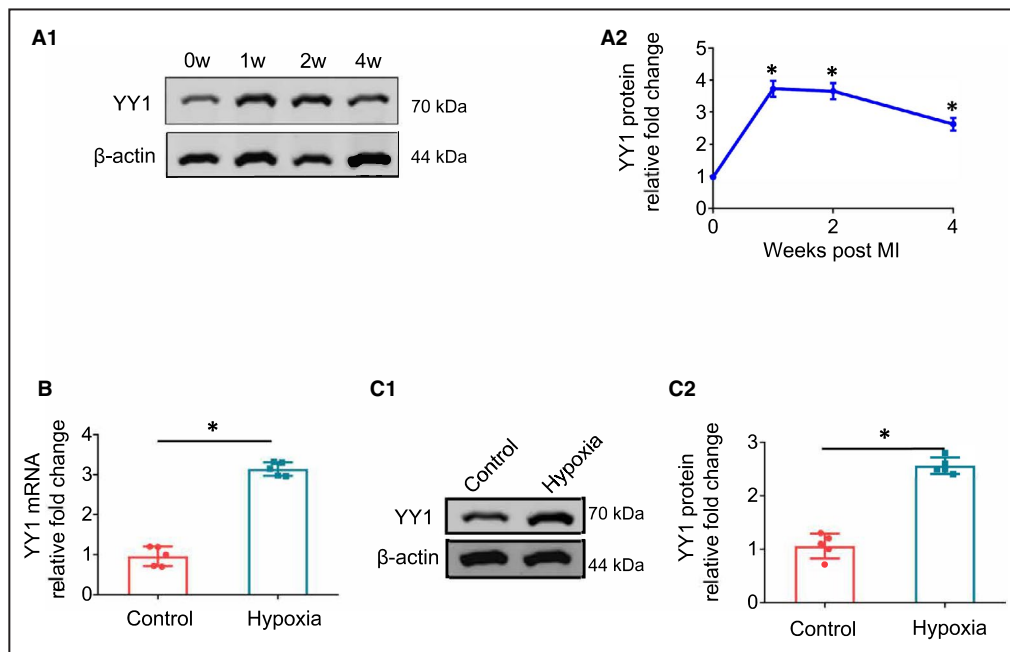


**Figure 1. YY1 expression was increased in the mouse heart after MI.**

**A1** and **A2**, The YY1 protein levels in the mouse heart at the indicated time point following MI, \**P*<0.05 vs sham at day 0, n=4. **B**, **C1**, and **C2**, YY1 mRNA and protein levels in cultured NRVMs subjected to hypoxia treatment (1% O<sub>2</sub>, for 24 hours), \**P*<0.05, n=5. MI indicates myocardial infarction; NRVM, neonatal rat ventricular myocyte; and YY1, Yin-Yang 1.

both the mRNA and protein expression of YY1 were induced by hypoxia in NRVMs (Figure 1B and 1C). These results indicated that YY1 levels in heart were elevated after MI, which may play a role in the pathological progression of ischemic myocardium injury.

### **Elevated YY1 Ameliorated Cardiac Remodeling After MI**

To explore whether YY1 participate in cardiac remodeling after MI, we injected AAV9-YY1 into the injured myocardium. The over-expression of YY1 was validated by western blot (Figure 2A). YY1 overexpression significantly improved the survival rate of mice following MI (Figure 2B). The ratios of heart weight to body weight and infarct size were remarkably reduced by AAV9-YY1 at 4 weeks after MI (Figure 2C and 2D). The improved left ventricular ejection fraction, and the reduced diastolic left ventricular internal diameter of mouse heart were also observed in AAV9-YY1 group (Figure 2E). On the other hand, silencing of YY1 by AAV9-shYY1 delivery deteriorated the survival, cardiac function and remodeling after MI (Figure 2F through 2J). These results indicated that YY1 is engaged in the cardiac remodeling after MI.

### **YY1 Inhibited Cardiomyocyte Apoptosis In Vivo and In Vitro**

Cell loss caused by acute and sustained hypoxia after MI is the pathological basis of cardiac remodeling. YY1 has been reported repressing apoptosis in cancer cells,<sup>8,9</sup> but whether or not it affect cardiomyocyte apoptosis in MI is unknown. Our data showed that in the border zone of the infarcted myocardium, terminal deoxynucleotidyl transferase mediated dUTP-biotin nick end labeling positive cardiomyocytes were reduced by AAV9-YY1, but increased by AAV9-shYY (Figure 3A). The cleaved caspase 3, an indicator of apoptosis,<sup>10</sup> was also significantly decreased by YY1 overexpression while augmented by YY1 silencing (Figure 3B). Similar results were observed in NRVMs subjected to hypoxia treatment (Figure S1). These data suggested that YY1 inhibits cardiomyocyte apoptosis in MI.

### **YY1 Promoted VEGF Levels and Angiogenesis in Infarcted Heart**

Previous studies revealed that YY1 plays an essential role in angiogenesis in a VEGF-dependent manner in tumors.<sup>4</sup> We evaluated the angiogenesis in the infarcted heart by staining endothelium marker CD31.<sup>11</sup> The CD31-positive vessel density was remarkably increased in AAV9-YY1 but decreased in AAV9-shYY1 groups (Figure 4A1 and 4A2). We next examined the effect of YY1 on migration and tube forming ability of endothelial cells as they are essential for angiogenesis.

The data showed that YY1 overexpression increased, while YY1 silencing repressed the migration in human umbilical vein endothelial cells (Figure S2). Similarly, matrigel-based tube formation assay indicated that the vessel like structure formation of human umbilical vein endothelial cells is promoted by YY1 overexpression but hampered by YY1 silencing (Figure 4B). The VEGF-A levels were measured by ELISA in both serum and infarcted myocardium 2 weeks after MI; increased VEGF-A level was observed in infarcted myocardium in AAV9-YY1 group (Figure 4C1), while the VEGF-A levels in serum were not changed (Figure 4C2). These results suggesting YY1 promotes VEGF-A levels and angiogenesis in infarcted heart.

### **YY1 Ameliorated Fibrosis in Post-MI Heart**

The expanded cardiac fibrosis post MI are detrimental as they lead to progressive impairment of cardiac function and eventually to heart failure.<sup>12</sup> Given that YY1 attenuates interstitial fibrosis in dilated cardiomyopathy,<sup>13</sup> we assessed whether the cardiac fibrosis is also regulated in the post-MI heart. Masson trichrome staining showed that YY1 overexpression limited the percentage of fibrosis area both in interstitial border zone and in the infarcted region of the mouse heart after MI, as compared with control (Figure S3).

### **YY1 Enhanced Akt Phosphorylation and VEGF-A Production**

Since the regulatory effects of YY1 on angiogenesis and apoptosis are dependent on Akt phosphorylation,<sup>14,15</sup> we wonder if YY1 regulates Akt phosphorylation in the post-MI heart. We found that the phospho-Akt levels were remarkably increased by YY1 overexpression, but repressed by YY1 silencing in mouse heart, while the total amount of Akt was not changed (Figure 5A). Similar results were obtained in VEGF-A levels in the border zone of the infarcted myocardium (Figure 5B). Given the VEGF-A is also regulated by Akt,<sup>16</sup> we explored if YY1 boost VEGF-A in an Akt dependent manner, and found that both in NRVMs and conditioned medium, YY1 overexpression increased VEGF-A production, and this is hampered by addition of Akt inhibitor, MK2206<sup>17</sup> (Figure 5C and 5D). These data together indicated that Akt phosphorylation and the subsequent VEGF-A elevation may contribute to the protective role of YY1 in the post-MI heart.

### **Akt Phosphorylation is Essential for YY1's Regulatory Effect on Apoptosis and Angiogenesis**

To explore the role of Akt in YY1's cardioprotective effects, the cardiomyocyte apoptosis and angiogenesis capability of endothelial cells were assessed with YY1

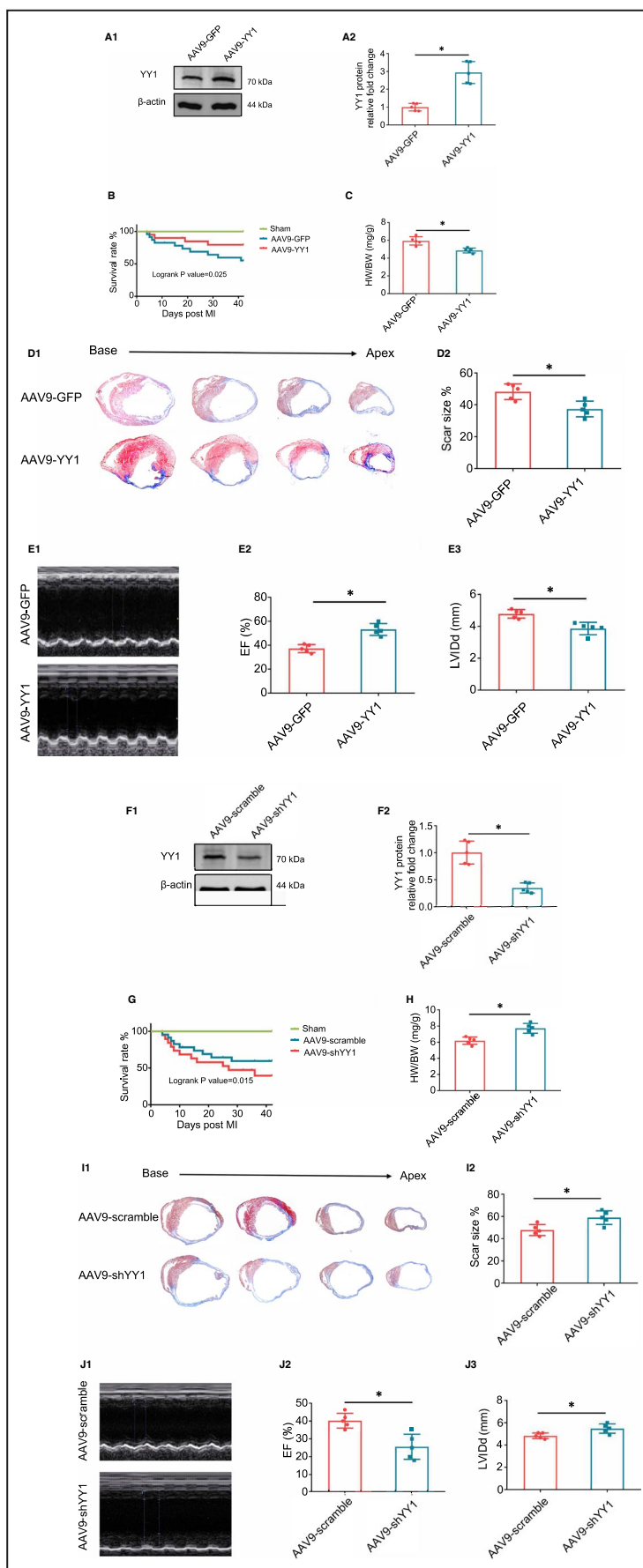


**Figure 2. YY1 ameliorated cardiac remodeling in the post-MI heart.**

**A1 and A2,** The representative western blot image (**A1**) and statistical result (**A2**) of YY1 at 4 weeks after MI in the mouse heart with intramyocardial AAV9-GFP or AAV9-YY1 delivery, \**P*<0.05, n=5. **B,** The survival rate of mice in indicated groups, n=15 to 20, the significance was analyzed by log-rank test and the *P* value was indicated. **C,** The ratio of heart weight to body weight (HW/BW), \**P*<0.05, n=5. **D1 and D2,** The representative image (**D1**) of Masson's trichrome staining of heart section (left to right: from base to apex) and statistical result (**D2**) of scar size, \**P*<0.05, n=5. **E1 through E3,** The representative M-mode echocardiography (**E1**), statistical result of EF (**E2**) and LVIDd (**E3**) of mouse heart, \**P*<0.05, n=5. **F1 and F2,** The representative western blot image (**F1**) and statistical result (**F2**) of YY1 in mouse at 4 weeks after MI in mouse heart with intramyocardial AAV9-scramble or AAV9-shYY1 delivery, \**P*<0.05, n=5. **G,** The survival rate of mice in indicated groups, n=14 to 19, the significance was analyzed by the log-rank test and the *P* value was indicated. **H,** The ratio of heart weight to body weight, \**P*<0.05, n=5. **I1 and I2,** The representative image (**I1**) of Masson's trichrome staining of heart section (left to right: from base to apex) and statistical result (**I2**) of scar size, \**P*<0.05, n=5. **J1 through J3,** The representative M-mode echocardiography (**J1**), statistical result of EF (**J2**) and diastolic left ventricular internal diameter (**J3**) of mouse heart, \**P*<0.05, n=5. AAV9 indicates adeno-associated virus 9; EF, ejection fraction; GFP, green fluorescent protein; LVIDd, diastolic left ventricular internal diameter; MI, myocardial infarction; shYY1, short hairpin Yin-Yang 1; and YY1, Yin-Yang 1.

overexpression plus Akt inhibition. In cultured NRMVs subjected to hypoxia treatment, the rescued apoptosis by YY1 overexpression was hampered by addition of MK2206 (Figure 6A). Similarly, the tube formation ability and migration ability of human umbilical vein

endothelial cells, were increased by YY1 overexpression, but neutralized by MK2206 (Figure 6B and 6C). These results suggested that the enhanced Akt phosphorylation is substantial for the repressed apoptosis and boosted angiogenesis by YY1 overexpression.

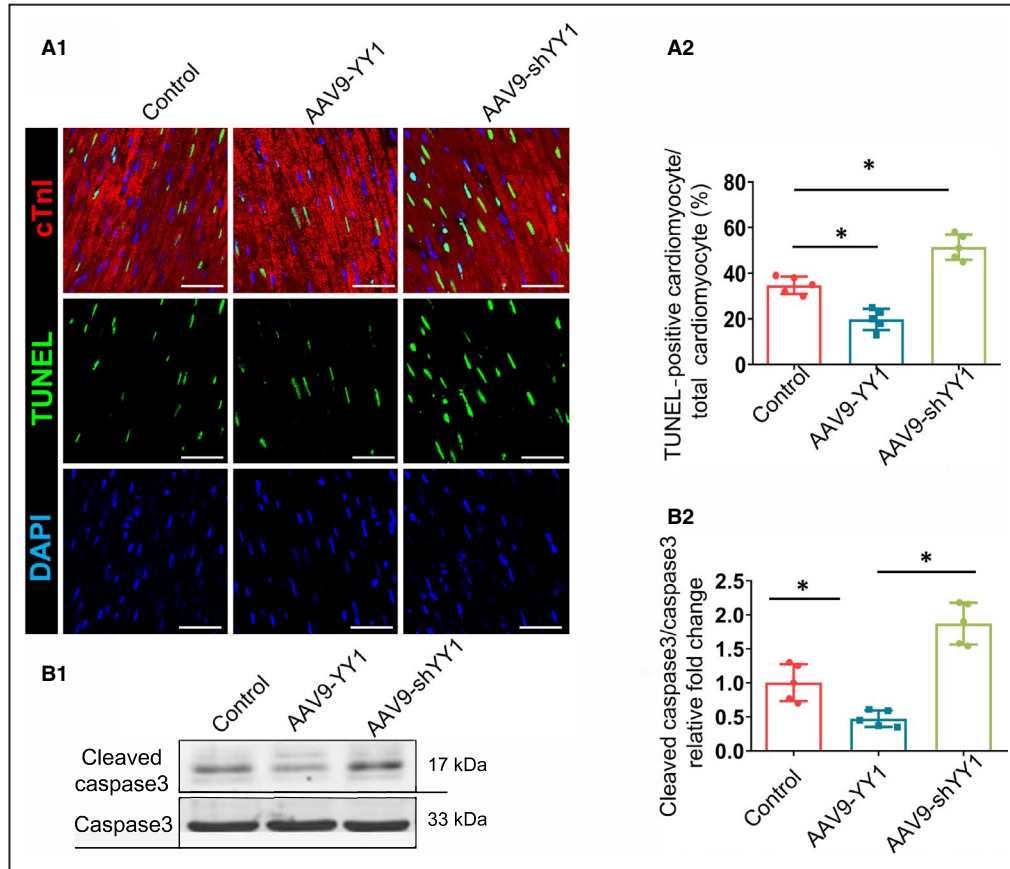


**Figure 3. YY1 inhibited cardiomyocyte apoptosis and caspase 3 cleavage.**

**A1 and A2,** The representative image (**A1**) and statistical result (**A2**) of TUNEL positive cardiomyocytes in heart 5 days after MI with AAV9-mediated YY1 over-expression (AAV9-YY1) or silencing (AAV9-shYY1), \**P*<0.05, n=6, scale bar=50 μm. **B1 and B2,** The representative image (**B1**) and statistical result (**B2**) of the cleaved-caspase3 protein levels in heart 5 days post-MI with AAV9 mediated YY1 over-expression (AAV9-YY1) or silencing (AAV9-shYY1), \**P*<0.05, n=6. cTnI indicates cardiac troponin I. AAV9 indicates adeno-associated virus 9; GFP, green fluorescent protein; LVIDd, diastolic left ventricular internal diameter; MI, myocardial infarction; shYY1, short hairpin Yin-Yang 1; TUNEL, terminal deoxynucleotidyl transferase mediated dUTP-biotin nick end labeling; VEGF-A, vascular endothelial growth factor A; and YY1, Yin-Yang 1.

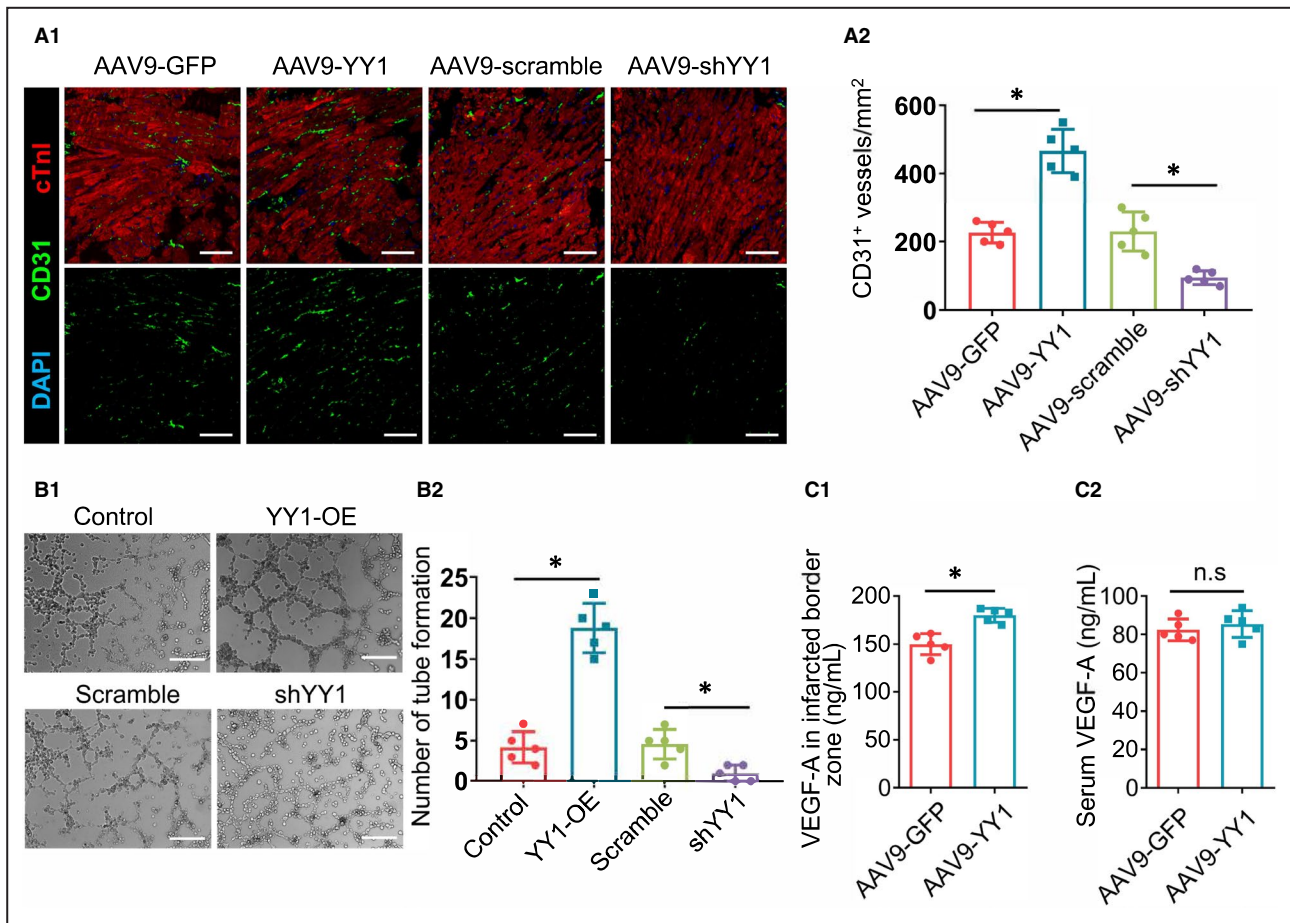


**Figure 4. YY1 promoted angiogenesis in the post-MI heart.** **A1** and **A2**, The representative image (**A1**) and statistical result (**A2**) of CD31-positive vessel density in myocardium 2 weeks after MI in AAV9-YY1/AAV9-GFP and AAV9-scramble/AAV9-shYY1 groups, \* $P < 0.05$ ,  $n = 5$ , scale bar = 50  $\mu\text{m}$ . **B1** and **B2**, The representative image (**B1**) and statistical result (**B2**) of vessel-like structure formed by HUVECs with or without YY1 overexpression (YY1-OE)/YY1 silencing (shYY1) in matrigel based tube formation assay, \* $P < 0.05$ ,  $n = 5$ , scale bar = 50  $\mu\text{m}$ . **C1** and **C2**, The statistical result of VEGF-A levels in mouse heart (**C1**) and in serum (**C2**) 2 weeks post MI in AAV9-YY1 and AAV9-GFP groups, \* $P < 0.05$ , n.s. indicates non-significant,  $n = 5$ . AAV9 indicates adeno-associated virus 9; GFP, green fluorescent protein; MI, myocardial infarction; shYY1, short hairpin Yin-Yang 1; TUNEL, terminal deoxynucleotidyl transferase mediated dUTP-biotin nick end labeling; VEGF-A, vascular endothelial growth factor A; and YY1, Yin-Yang 1.

### YY1 Promoted T Helper 2 Cytokines Production and M2 Macrophage Polarization Post MI

It is previously reported that YY1 activates the T helper 2 lymphocyte (Th2)-specific transcription factor GATA binding protein 3<sup>18</sup> and thus promotes Th2 differentiation as well as Th2 cytokines interleukin-4, interleukin-5 and interleukin-13 production in lymphocyte.<sup>19</sup> As these Th2 cytokines are considered protective against MI,<sup>20</sup> we explored whether they are also affected by YY1 in the post-MI heart. Our results showed that YY1 overexpression significantly increased GATA binding protein 3 mRNA levels, and the mRNA and protein levels of interleukin-4, interleukin-5, and interleukin-13 in the post-MI heart (Figure S4).

Since the cardioprotective effect of Th2 cytokines are partially through the polarization of M2 macrophages,<sup>21</sup> we investigated whether M2 polarization is indeed regulated by YY1 in the post-MI heart. Immunostaining and western blot for pan-macrophage marker CD68<sup>22</sup> demonstrated that the overall macrophage infiltration was unchanged by YY1 overexpression (Figure S5A, S5B1, and S5B9), but a significant elevation in protein levels of M2 markers CD163, arginase-1, and interleukin-10,<sup>23</sup> along with the reduction in that of the M1 makers CD86, interleukin-1 $\beta$ , and inducible nitric oxide synthase<sup>23</sup> were observed in the YY1 overexpression group as compared with control (Figure S5B1 through S5B8).

These data together indicated that YY1 promotes Th2 cytokines production and M2 macrophage



polarization, which might be involved in the mechanisms underlying the cardioprotective effect of YY1.

## DISCUSSION

YY1 is a ubiquitous and multifunctional zinc-finger transcription factor and belongs to the polycomb group protein family. It regulates varieties of genes involved in cell cycle, apoptosis, oncogenesis, and angiogenesis.<sup>4,24</sup> There are reports showing that YY1 is involved in heart development and cardiovascular diseases. For example, YY1 promotes mesodermal cardiac differentiation as a transcriptional activator of *Nkx2.5*.<sup>25</sup> YY1 protects cardiomyocytes from hypertrophy by binding to histone deacetylase 5 and preventing its clear export.<sup>6</sup> The expression and activity of YY1 were increased in the human failing heart,<sup>5</sup> but its role in MI is unclear.

Cell loss caused by MI is the pathological basis of cardiac remodeling. A wealth of experimental data has

linked YY1 to cell apoptosis. Ablation of YY1 increases apoptosis in germinal center B cells and Hela cells.<sup>9,26</sup> Negative regulation of p53 and Fas receptor by YY1 is involved in its inhibitory effects on apoptosis.<sup>8,9,27</sup> Whether YY1 participates in apoptosis in the post-MI heart remains unclear. In the present study, we found that overexpression of YY1 ameliorated cardiomyocyte apoptosis, which might contribute to the protective role of YY1 in MI.

Therapeutic angiogenesis emerged as a potential treatment for MI patients.<sup>28</sup> The proangiogenesis effect of YY1 has been explored in tumor growth and metastasis.<sup>29</sup> The stimulatory effect of YY1 on angiogenesis is dependent on VEGF production.<sup>30</sup> YY1 promotes VEGF production by either binding to the VEGF gene promoter or enhancing Akt phosphorylation.<sup>16,29,30</sup> Notably, the regulatory effect of YY1 on angiogenesis in ischemic myocardium has not been explored before. Our data demonstrated that YY1 enhanced the angiogenesis and VEGF production either in infarcted

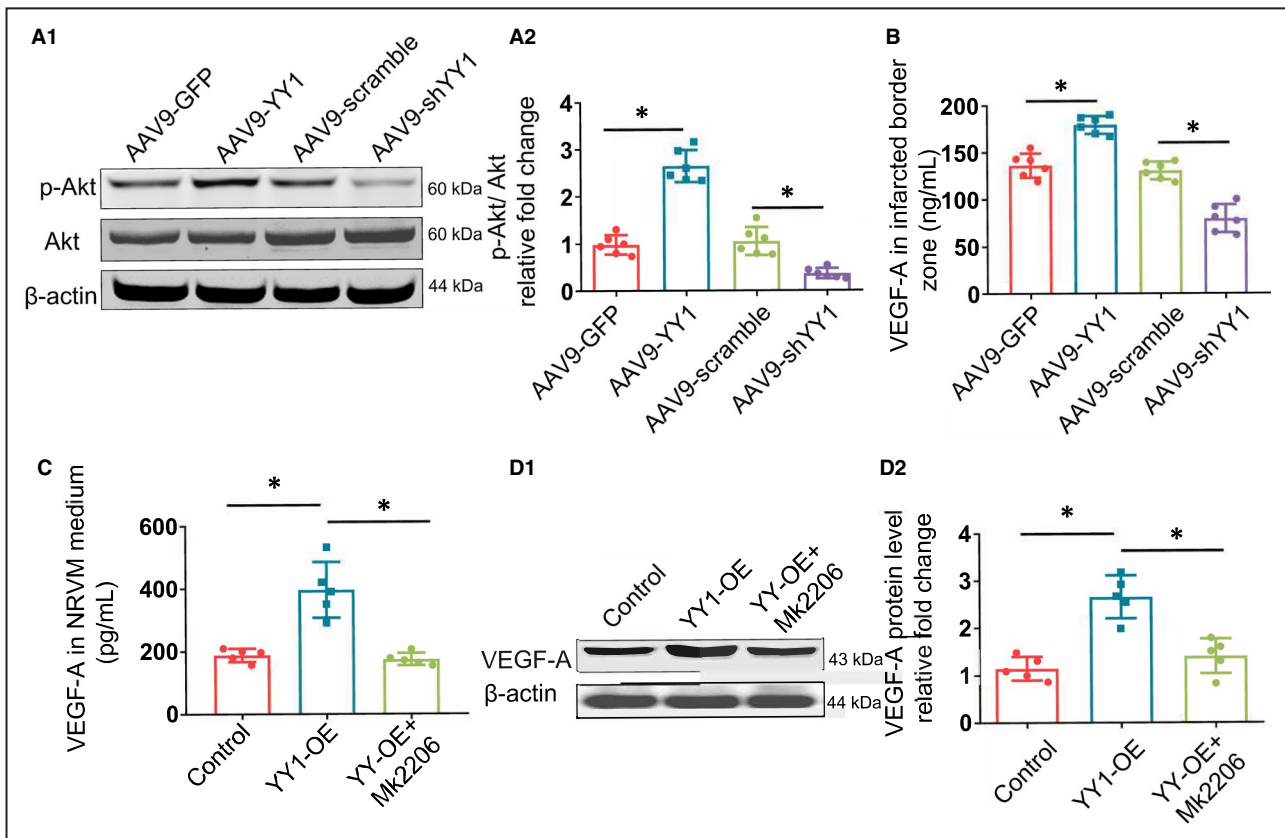
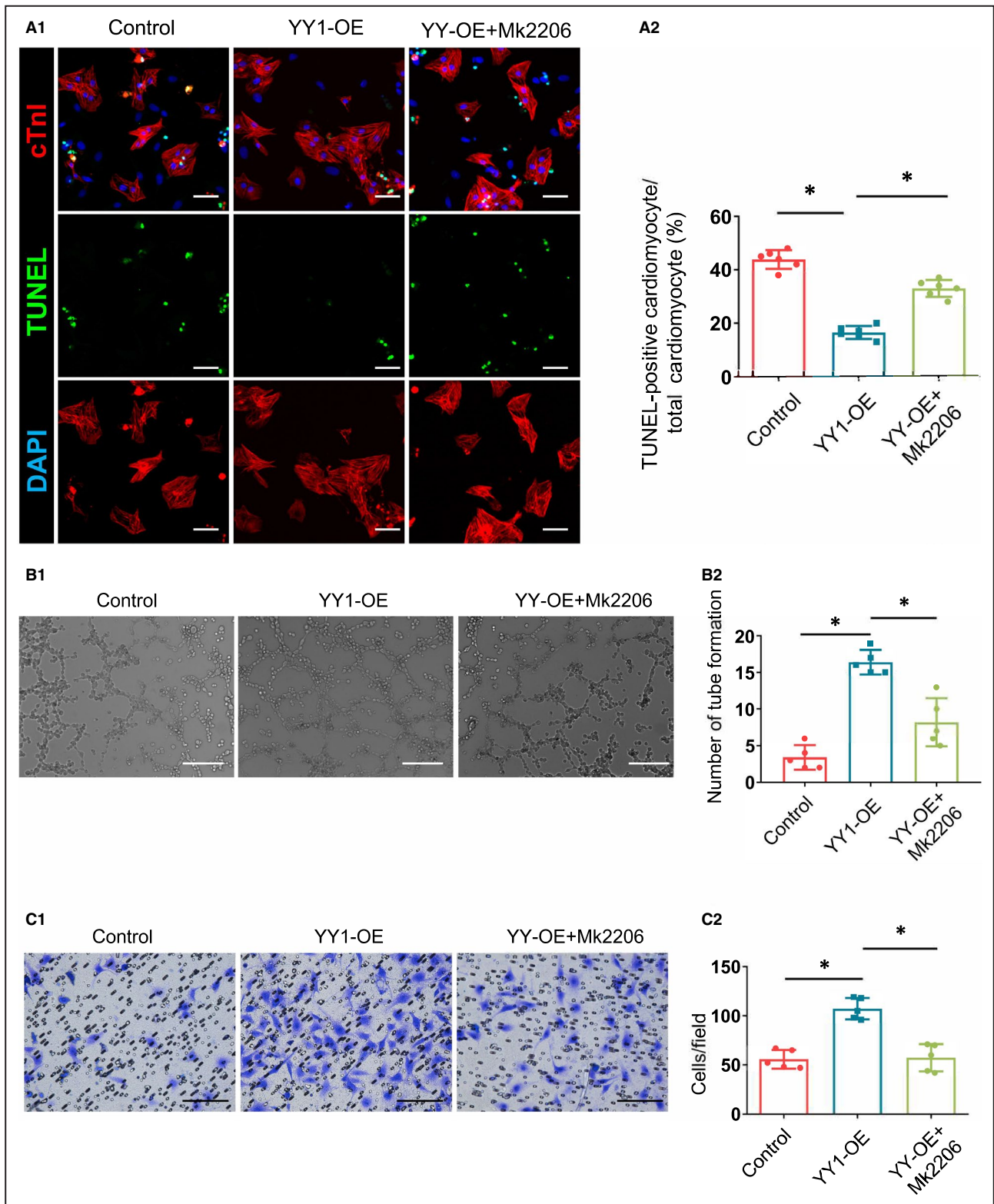


**Figure 5. YY1 increased Akt phosphorylation and VEGF-A levels in post-MI heart.**

**A1** and **A2**, The protein levels of total Akt, phosphorylated Akt, and β-actin in mouse heart 2 weeks post-MI, with AAV9 mediated YY1 over-expression (AAV9-YY1) or silencing (AAV9-shYY1), \**P*<0.05, n=6. **B**, The VEGF-A levels detected by ELISA in infarct border zone from mouse heart 2 weeks after MI, with AAV9 mediated YY1 overexpression (AAV9-YY1) or silencing (AAV9-shYY1), \**P*<0.05, n=6. **C**, The VEGF-A levels detected by ELISA at 48 hours in cultured medium of NRVM with YY1 over-expression (YY1-OE) or YY1-OE plus Akt inhibitor MK2206 treatment (3 μmol/L), \**P*<0.05, n=5. **D1** and **D2**, The VEGF-A levels detected by western blot at 48 hours in NRVM with YY1 overexpression (YY1-OE) or YY1-OE plus Akt inhibitor MK2206 treatment (3 μmol/L) \**P*<0.05, n=5. AAV9 indicates adeno-associated virus 9; GFP, green fluorescent protein; MI, myocardial infarction; NRVM, neonatal rat ventricular myocyte; shYY1, short hairpin Yin-Yang 1; VEGF-A, vascular endothelial growth factor A; and YY1, Yin-Yang 1.



myocardium or in cultured endothelial cells, supporting an important role of angiogenesis in YY1's protective effect against MI.

A previous study reported that in a dilated cardiomyopathy model in the mouse induced by lamin A

deficiency, overexpression of YY1 suppressed the progression of dilated cardiomyopathy and the interstitial cardiac fibrosis by up-regulating Bmp7 and repressing connective tissue growth factor.<sup>13</sup> Accordingly, we found that in the context of MI, cardiac fibrosis is also inhibited

**Figure 6. YY1 inhibited apoptosis and promoted angiogenesis in an Akt-dependent way.**

**A1** and **A2**, The representative image (**A1**) and statistical result (**A2**) of TUNEL-positive NRVMs subjected to hypoxia treatment (1% O<sub>2</sub> for 24 hours) with YY1 overexpression (YY1-OE) or YY1-OE plus Akt inhibitor MK2206 treatment (3 μmol/L), \**P*<0.05, n=6, scale bar=50 μm. **B1** and **B2**, The representative image (**B1**) and statistical result (**B2**) of vessel-like structure formed by human umbilical vein endothelial cells with YY1 over-expression (YY1-OE) or YY1-OE plus Akt inhibitor MK2206 treatment (3 μmol/L) in matrigel based tube formation assay, \**P*<0.05, n=5, scale bar=50 μm. **C1** and **C2**, The representative image (**C1**) and statistical result (**C2**) of crystal violet staining of migrated human umbilical vein endothelial cells transfected with YY1 overexpression (YY1-OE) or YY1-OE plus Akt inhibitor MK2206 treatment (3 μmol/L). \**P*<0.05, n=5, scale bar=50 μm. cTnl indicates cardiac troponin I; NRVM, neonatal rat ventricular myocyte; TUNEL, terminal deoxynucleotidyl transferase mediated dUTP-biotin nick end labeling; and YY1, Yin-Yang 1.

by YY1 overexpression. The regulatory effect of YY1 on fibrosis in other cardiovascular disease model, particularly in heart failure with preserved ejection fraction is worthy of further investigation, given the central role of fibrosis in heart failure with preserved ejection fraction.

Inflammatory responses also play a regulatory role in cardiac remodeling following MI, among which lymphocytes and macrophages are most studied.<sup>31</sup> Interleukin-4, interleukin-5, and interleukin-13 are Th2 lymphocyte cytokines and have been reported to protect the heart from MI. These cytokines facilitate the recruitment and polarization of M2 macrophages (interleukin-4),<sup>21,32,33</sup> and enhance cardiac regeneration by stimulation of signal transducer and activator of transcription signaling (interleukin-13).<sup>34,35</sup> A previous study reported that YY1 promotes Th2 lymphocyte differentiation as well as Th2 cytokine induction.<sup>19</sup> Our data revealed that overexpression of YY1 stimulated interleukin-4, interleukin-5, and interleukin-13 production in the post-MI heart. Accordingly, a polarization shift toward the M2 macrophage phenotype was also observed along with YY1 overexpression, as evidenced by the increased optimal M2 marker CD163, arginase-1, and interleukin-10, and the decreased M1 marker CD86, interleukin-1β, and inducible nitric oxide synthase. In contrast to proinflammatory M1 macrophage, M2 macrophage are recognized as anti-inflammatory and reparative for MI.<sup>36</sup> These alteration may also account for the cardioprotective effect of YY1.

Finally, we examined the mechanisms underlying the protective effect of YY1 against MI. Akt signal pathway is an important one for inhibition of cell apoptosis and stimulation of angiogenesis. Several lines of evidence suggested that YY1 promotes Akt phosphorylation at serine 473 in cancer cells, which is considered as a marker of Akt activation.<sup>37</sup> Given the importance of Akt phosphorylation on apoptosis and angiogenesis, we examined their alteration with YY1 manipulation. It showed that YY1 significantly enhanced Akt phosphorylation in post-MI heart. Akt inhibitor, MK2206 blocked the elevated VEGF-A production, alleviated cardiomyocyte apoptosis and enhanced endothelial cell migration as well as tube formation ability induced by YY1. Therefore, we envisaged that Akt phosphorylation may be the underlying mechanisms accounting for the protective effect of YY1 against MI.

In summary, we first demonstrated that YY1 is increased in the post-MI heart, and that overexpression of YY1 ameliorates cardiac injury and remodeling by repressing cardiomyocyte apoptosis, boosting angiogenesis, and activating Th2 lymphocyte and M2 macrophages. This is possibly attributable to the enhancement of Akt phosphorylation and the subsequent VEGF up-regulation. Our findings extended the role of YY1 in heart and supported YY1 as a potent therapeutic target for treating MI.

**ARTICLE INFORMATION**

Received April 1, 2021; accepted September 15, 2021.

**Affiliations**

Department of Cardiology, Daping Hospital (Y.H., L.L., H.C., Q.L., X.Y., D.Y., X.X., H.W., W.E.W., C.Z.) and State Key Laboratory of Trauma, Burns and Combined Injury (C.Z.), Third Military Medical University, Chongqing, P. R. China Chongqing Key Laboratory for Hypertension Research, Chongqing Cardiovascular Clinical Research Center, Chongqing Institute of Cardiology, Chongqing, P. R. China (L.L., H.C., Q.L., X.Y., D.Y., X.X., H.W., W.E.W., C.Z.); Department of Cardiology of Chongqing General Hospital, Cardiovascular Research Center of Chongqing College, University of Chinese Academy of Sciences, Chongqing, P. R. China (C.Z.); and Department of Cardiology, Fujian Heart Medical Center, Fujian Institute of Coronary Heart Disease, Fujian Medical University Union Hospital, Fuzhou, P. R. China (Y.H., L.C., C.Z.).

**Sources of Funding**

This work was supported by grants from the National Natural Science Foundation of China (81930008, 81922005, 81600230), National Key R&D Program of China (2018YFC1312700), Program of Innovative Research Team by National Natural Science Foundation (81721001), and Key Project of Chongqing Fundamental Science and Frontier Technology Research (cstc2015cyjBX0129).

**Disclosures**

None.

**Supplementary Material**

Data S1  
Figures S1–S5

**REFERENCES**

1. Reed GW, Rossi JE, Cannon CP. Acute myocardial infarction. *Lancet*. 2017;389:197–210. doi: 10.1016/S0140-6736(16)30677-8
2. Li M, Izzipua Belmonte JC. Mending a faltering heart. *Circ Res*. 2016;118:344–351. doi: 10.1161/CIRCRESAHA.115.306820
3. Su J, Sui YI, Ding J, Li F, Shen S, Yang Y, Lu Z, Wang F, Cao L, Liu X, et al. Human INO80/YY1 chromatin remodeling complex transcriptionally regulates the BRCA2- and CDKN1A-interacting protein (BCCIP) in cells. *Protein Cell*. 2016;7:749–760. doi: 10.1007/s13238-016-0306-1
4. Wu S, Kasim V, Kano MR, Tanaka S, Ohba S, Miura Y, Miyata K, Liu X, Matsuhashi A, Chung UI, et al. Transcription factor YY1 contributes

- to tumor growth by stabilizing hypoxia factor HIF-1 $\alpha$  in a p53-independent manner. *Cancer Res.* 2013;73:1787–1799.
5. Sucharov CC, Mariner P, Long C, Bristow M, Leinwand L. Yin Yang 1 is increased in human heart failure and represses the activity of the human  $\alpha$ -myosin heavy chain promoter. *J Biol Chem.* 2003;278:31233–31239.
  6. Sucharov CC, Dockstader K, McKinsey TA. YY1 protects cardiac myocytes from pathologic hypertrophy by interacting with HDAC5. *Mol Biol Cell.* 2008;19:4141–4153. doi: 10.1091/mbc.e07-12-1217
  7. Wang WE, Li L, Xia X, Fu W, Liao Q, Lan C, Yang D, Chen H, Yue R, Zeng C, et al. Dedifferentiation, proliferation, and redifferentiation of adult mammalian cardiomyocytes after ischemic injury. *Circulation.* 2017;136:834–848. doi: 10.1161/CIRCULATIONAHA.116.024307
  8. Sui G, Affar el B, Shi Y, Brignone C, Wall NR, Yin P, Donohoe M, Luke MP, Calvo D, Grossman SR, et al. Yin Yang 1 is a negative regulator of p53. *Cell.* 2004;117:859–872. doi: 10.1016/j.cell.2004.06.004
  9. Gronroos E, Terentiev AA, Punga T, Ericsson J. YY1 inhibits the activation of the p53 tumor suppressor in response to genotoxic stress. *Proc Natl Acad Sci U S A.* 2004;101:12165–12170. doi: 10.1073/pnas.0402283101
  10. Sharma AK, Rohrer B. Calcium-induced calpain mediates apoptosis via caspase-3 in a mouse photoreceptor cell line. *J Biol Chem.* 2017;292:13186.
  11. Liu L, Shi GP. CD31: beyond a marker for endothelial cells. *Cardiovasc Res.* 2012;94:3–5. doi: 10.1093/cvr/cvs108
  12. Talman V, Ruskoaho H. Cardiac fibrosis in myocardial infarction—from repair and remodeling to regeneration. *Cell Tissue Res.* 2016;365:563–581. doi: 10.1007/s00441-016-2431-9
  13. Tan CY, Wong JX, Chan PS, Tan H, Liao D, Chen W, Tan LW, Ackers-Johnson M, Wakimoto H, Seidman JG, et al. Yin Yang 1 suppresses dilated cardiomyopathy and cardiac fibrosis through regulation of *Bmp7* and *Ctgf*. *Circ Res.* 2019;125:834–846.
  14. Zhang X, Tang N, Hadden TJ, Rishi AK. Akt, FoxO and regulation of apoptosis. *Biochim Biophys Acta.* 2011;1813:1978–1986. doi: 10.1016/j.bbamcr.2011.03.010
  15. Jiang BH, Liu LZ. Akt signaling in regulating angiogenesis. *Curr Cancer Drug Targets.* 2008;8:19–26.
  16. Pore N, Liu S, Shu H-K, Li B, Haas-Kogan D, Stokoe D, Milanini-Mongiati J, Pages G, O'Rourke DM, Bernhard E, et al. Sp1 is involved in Akt-mediated induction of VEGF expression through an HIF-1-independent mechanism. *Mol Biol Cell.* 2004;15:4841–4853. doi: 10.1091/mbc.e04-05-0374
  17. Liu J, Duan Z, Guo W, Zeng L, Wu Y, Chen Y, Tai F, Wang Y, Lin Y, Zhang Q, et al. Targeting the BRD4/FOXO3a/CDK6 axis sensitizes AKT inhibition in luminal breast cancer. *Nat Commun.* 2018;9:5200. doi: 10.1038/s41467-018-07258-y
  18. Yan X, Zhang H, Fan Q, Hu J, Tao R, Chen Q, Iwakura Y, Shen W, Lu L, Zhang QI, et al. Dectin-2 deficiency modulates Th1 differentiation and improves wound healing after myocardial infarction. *Circ Res.* 2017;120:1116–1129. doi: 10.1161/CIRCRESAHA.116.310260
  19. Hwang SS, Kim YU, Lee S, Jang SW, Kim MK, Koh BH, Lee W, Kim J, Souabni A, Busslinger M, et al. Transcription factor YY1 is essential for regulation of the Th2 cytokine locus and for Th2 cell differentiation. *Proc Natl Acad Sci U S A.* 2013;110:276–281. doi: 10.1073/pnas.1214682110
  20. Cheng X, Liao Y-H, Ge H, Li B, Zhang J, Yuan J, Wang M, Liu Y, Guo Z, Chen J, et al. Th1/Th2 functional imbalance after acute myocardial infarction: coronary arterial inflammation or myocardial inflammation. *J Clin Immunol.* 2005;25:246–253. doi: 10.1007/s10875-005-4088-0
  21. Shintani Y, Ito T, Fields L, Shiraishi M, Ichihara Y, Sato N, Podaru M, Kainuma S, Tanaka H, Suzuki K. IL-4 as a repurposed biological drug for myocardial infarction through augmentation of reparative cardiac macrophages: proof-of-concept data in mice. *Sci Rep.* 2017;7:6877. doi: 10.1038/s41598-017-07328-z
  22. Loffler J, Sass FA, Filter S, Rose A, Ellinghaus A, Duda GN, Dienelt A. Compromised bone healing in aged rats is associated with impaired M2 macrophage function. *Front Immunol.* 2019;10:2443. doi: 10.3389/fimmu.2019.02443
  23. Liu M, Yin L, Li W, Hu J, Wang H, Ye B, Tang Y, Huang C. C1q/TNF-related protein-9 promotes macrophage polarization and improves cardiac dysfunction after myocardial infarction. *J Cell Physiol.* 2019;234:18731–18747. doi: 10.1002/jcp.28513
  24. Shi J, Hao A, Zhang Q, Sui G. The role of YY1 in oncogenesis and its potential as a drug target in cancer therapies. *Curr Cancer Drug Targets.* 2015;15:145–157.
  25. Gregoire S, Karra R, Passer D, Deutsch MA, Krane M, Feistritz R, Sturzu A, Domian I, Saga Y, Wu SM. Essential and unexpected role of Yin Yang 1 to promote mesodermal cardiac differentiation. *Circ Res.* 2013;112:900–910. doi: 10.1161/CIRCRESAHA.113.259259
  26. Trabucco SE, Gerstein RM, Zhang H. YY1 regulates the germinal center reaction by inhibiting apoptosis. *J Immunol.* 2016;197:1699–1707. doi: 10.4049/jimmunol.1600721
  27. Garban HJ, Bonavida B. Nitric oxide inhibits the transcription repressor Yin-Yang 1 binding activity at the silencer region of the Fas promoter: a pivotal role for nitric oxide in the up-regulation of Fas gene expression in human tumor cells. *J Immunol.* 2001;167:75–81. doi: 10.4049/jimmu.167.1.75
  28. Oostendorp M, Douma K, Wagenaar A, Slenter JM, Hackeng TM, van Zandvoort MA, Post MJ, Backes WH. Molecular magnetic resonance imaging of myocardial angiogenesis after acute myocardial infarction. *Circulation.* 2010;121:775–783. doi: 10.1161/CIRCULATIONAHA.109.889451
  29. de Nigris F, Crudele V, Giovane A, Casamassimi A, Giordano A, Garban HJ, Cacciatore F, Pentimalli F, Marquez-Garban DC, Petrillo A, et al. CXCR4/YY1 inhibition impairs VEGF network and angiogenesis during malignancy. *Proc Natl Acad Sci U S A.* 2010;107:14484–14489. doi: 10.1073/pnas.1008256107
  30. Petrella BL, Brinckerhoff CE. PTEN suppression of YY1 induces HIF-2 activity in von-Hippel-Lindau-null renal-cell carcinoma. *Cancer Biol Ther.* 2009;8:1389–1401. doi: 10.4161/cbt.8.14.8880
  31. Ong SB, Hernandez-Resendiz S, Crespo-Avilan GE, Mukhametshina RT, Kwek XY, Cabrera-Fuentes HA, Hausenloy DJ. Inflammation following acute myocardial infarction: multiple players, dynamic roles, and novel therapeutic opportunities. *Pharmacol Ther.* 2018;186:73–87. doi: 10.1016/j.pharmthera.2018.01.001
  32. Szkodziniski J, Hudzik B, Osuch M, Romanowski W, Szygula-Jurkiewicz B, Polonski L, Zubelewicz-Szkodziniska B. Serum concentrations of interleukin-4 and interferon-gamma in relation to severe left ventricular dysfunction in patients with acute myocardial infarction undergoing percutaneous coronary intervention. *Heart Vessels.* 2011;26:399–407. doi: 10.1007/s00380-010-0076-2
  33. Kanellakis P, Ditiatkovski M, Kostolias G, Bobik A. A pro-fibrotic role for interleukin-4 in cardiac pressure overload. *Cardiovasc Res.* 2012;95:77–85. doi: 10.1093/cvr/cvs142
  34. Hershey GK. IL-13 receptors and signaling pathways: an evolving web. *J Allergy Clin Immunol.* 2003;111:677–690; quiz 691. doi: 10.1067/mai.2003.1333
  35. O'Meara CC, Wamstad JA, Gladstone RA, Fomovsky GM, Butty VL, Shrikumar A, Gannon JB, Boyer LA, Lee RT. Transcriptional reversion of cardiac myocyte fate during mammalian cardiac regeneration. *Circ Res.* 2015;116:804–815. doi: 10.1161/CIRCRESAHA.116.304269
  36. Peet C, Ivetic A, Bromage DI, Shah AM. Cardiac monocytes and macrophages after myocardial infarction. *Cardiovasc Res.* 2020;116:1101–1112. doi: 10.1093/cvr/cvz336
  37. Zhang Q, Wan M, Shi J, Horita DA, Miller LD, Kute TE, Kridel SJ, Kulik G, Sui G. Yin Yang 1 promotes mTORC2-mediated AKT phosphorylation. *J Mol Cell Biol.* 2016;8:232–243. doi: 10.1093/jmcb/mjw002

# **SUPPLEMENTAL MATERIAL**

## **Data S1**

### **Supplemental Methods**

#### **1. Immunohistochemistry**

Mouse hearts were fixed and embedded in paraffin. 4  $\mu\text{m}$  sections were used for immunostaining. The sections were dewaxed and rehydrated, subjected to antigen retrieval (microwave for 15 min in 0.01 M sodium citrate (pH 6.0)), and blocked by donkey serum (Beyotime, Suzhou, China). The sections were incubated with cardiac troponin I antibody (cat# MA1-22700, Invitrogen, CA) or CD68 antibody (cat#28058-1-AP, Proteintech, Wuhan, China), and then recognized by Alexa Fluo<sup>®</sup> 546 conjugated secondary antibody (cat#A10040, Invitrogen, CA) or Alexa Fluo<sup>®</sup> 488 conjugated secondary antibody (cat#A-21202, Invitrogen, CA). TUNEL staining was performed using the in situ death detection kit (Beyotime, Suzhou, China). The nuclei was stained by 2-(4-Amidinophenyl)-6-indolecarbamide dihydrochloride (DAPI, Beyotime, Suzhou, China). Imaging was performed on a Fluoview 1000 confocal microscope (Olympus, Tokyo, Japan).

#### **2. Masson's trichrome staining and measurement of fibrosis.**

Mouse hearts (4 weeks post-MI) were fixed and embedded in paraffin, cut as 4  $\mu\text{m}$ -thick sections then dewaxed and rehydrated before use. Cardiac fibrosis was assessed by Masson's trichrome kit (Solarbio, Beijing, China) according to the manufactures' instruction. The percentage of fibrotic area of left ventricle was measured using Image J software (National Institutes of Health, MD).

#### **3. Cell migration Assay**

Cell migration was analyzed by a transwell migration assay. In brief, human umbilical vein endothelial cells (HUVECs) were transfected with YY1 over-expression plasmids or shRNA-against YY1 plasmids. 24 hours later,  $2.5 \times 10^4$  cells were plated into the top well of transwell migration chamber (Merck, Darmstadt, Germany). After 24 hours, the non-migrating cells were removed with a cotton swab, and the migrating cells on the underside of membrane were stained with crystal violet. Crystal violet positive cells were imaged under  $40 \times$  field with microscope (Nikon, Tokyo, Japan).

#### 4. Real time polymerase chain reaction (real-time PCR)

Total RNA was extracted from heart tissue with TRIzol (Invitrogen, NY) and purified with RNeasy kits (Qiagen, Hilden, Germany). After reverse transcription by reverse transcriptase (Takara, Kyoto, Japan), real-time PCR was performed using the SYBR Green Mastermix-Kit (Takara, Kyoto, Japan) and the CFX 96 real time PCR System (Bio-Rad, CA). Real-time PCR primers (Sangon, Shanghai, China) are as below:

Primer sets	Forward (5' ->3')	Reverse (5' ->3')
mIL-4	TCACAGCAACGAAGAACCAC	CGATGAATCCAGGCATCGAAAA
mIL-5	AATCAAAGTGTCCGTGGGGG	TCCTCGCCACACTTCTCTTTT
mIL-3	CACACAAGACCAGACTCCCCT	GCCATGCAATATCCTCTGGGT
mGATA3	GCTCCTTGCTACTCAGGTGAT	GGAGGGAGAGAGGAATCCGA
m18S rRNA	TTGACGGAAGGGCACCACCAG	GCACCACCACCCACGGAATCG

#### 5. Western blot

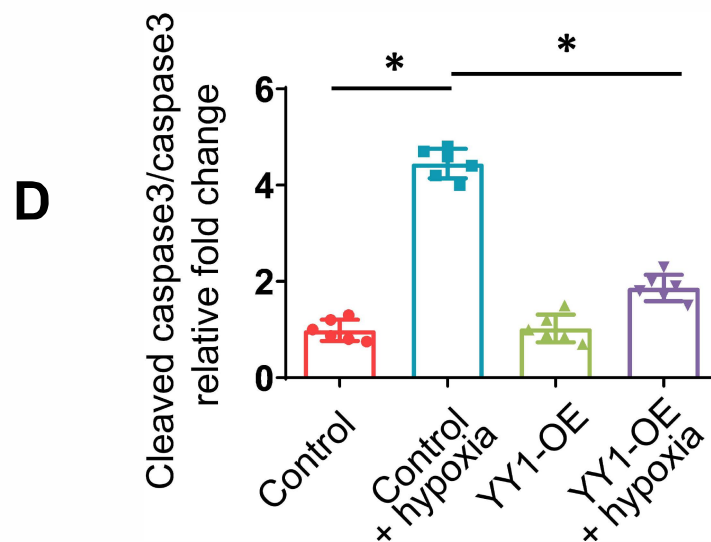
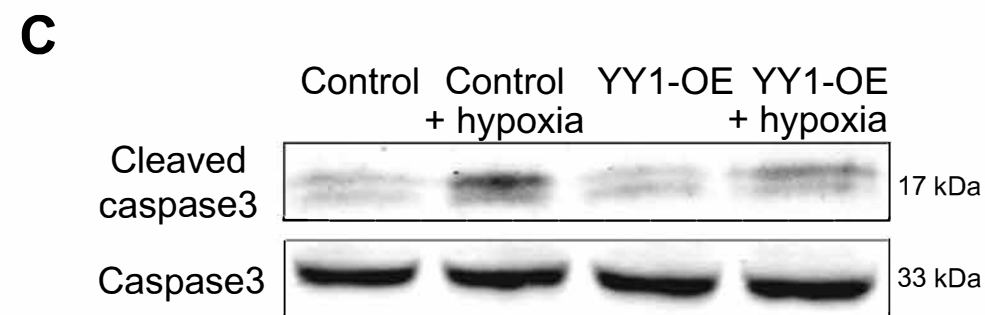
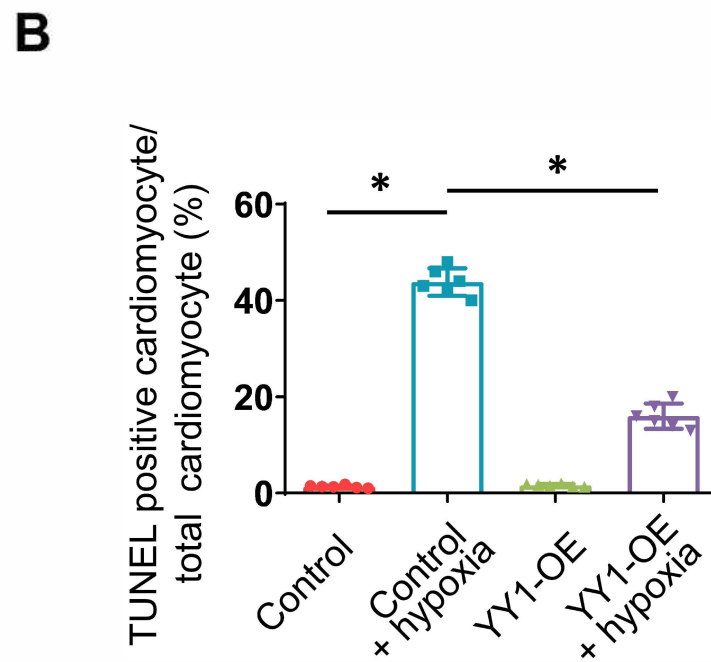
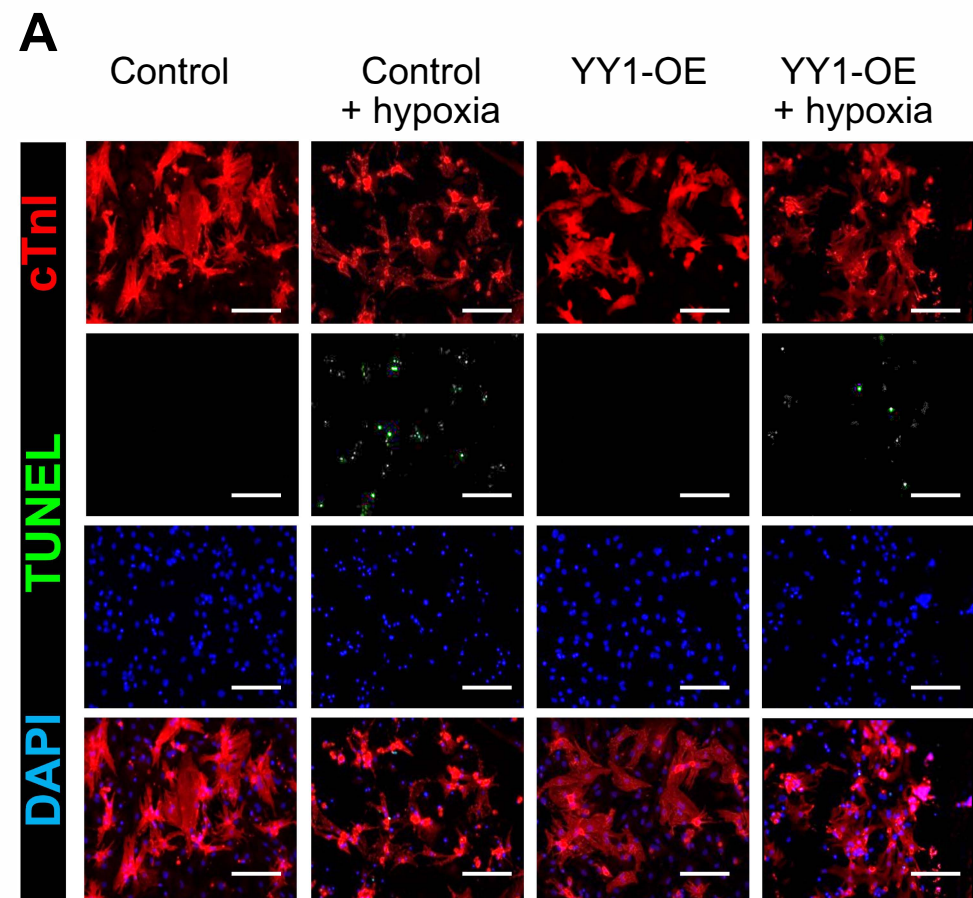
The total protein of mice heart were isolated using WB&IP lysis buffer containing 20mM Tris, 150mM NaCl, and 1% Triton X-100 (Beyotime, Suzhou, China) supplied with proteinase inhibitor cocktail and phosphatase inhibitor (Bimake, TX). Equal amount of 50µg proteins sample were separated by SDS-PAGE and transferred to polyvinylidene fluoride membranes (Bio-Rad, CA). The membranes were probed with YY1 antibody (cat# sc-7341, Santa Cruz, TX), IL-4, IL-5, and IL-13 antibody (cat#ER1706-55, cat# ER1911-38, cat# ER1911-23, Huabio, Hangzhou, China), CD163, CD86, CD68, IL-10, IL-1β, iNOS, Arginase-1 and β-actin antibody (cat#16646-1-AP, cat#13395-1-AP, cat#66231-2-Ig, cat#20850-1-AP, cat#16806-1-AP, cat#18985-1-AP, cat#16001-1-AP, cat#66009-1-Ig, Proteintech, Wuhan, China) respectively, and then recognized by CW800/RD680 fluorescence conjugated donkey anti rabbit/mouse IgG antibody (cat#926-68072, cat#925-32213, LI-COR Biosciences, NE). The membrane signal was scanned using Odyssey CLX Imager system (LI-COR Biosciences, NE). The densitometry values were normalized with β-actin protein signal.

#### 6. Statistical analyses.

Statistical analyses were performed by one-way analysis of variance (ANOVA) followed by Bonferroni's multiple comparison test (for comparison of more than two groups) or Student's t-test

(for comparison of two groups) (GraphPad Prism 8.0, GraphPad Software Inc, CA). Data are given as mean  $\pm$  SD, and a P value (two-sided) of  $<0.05$  was considered significant.

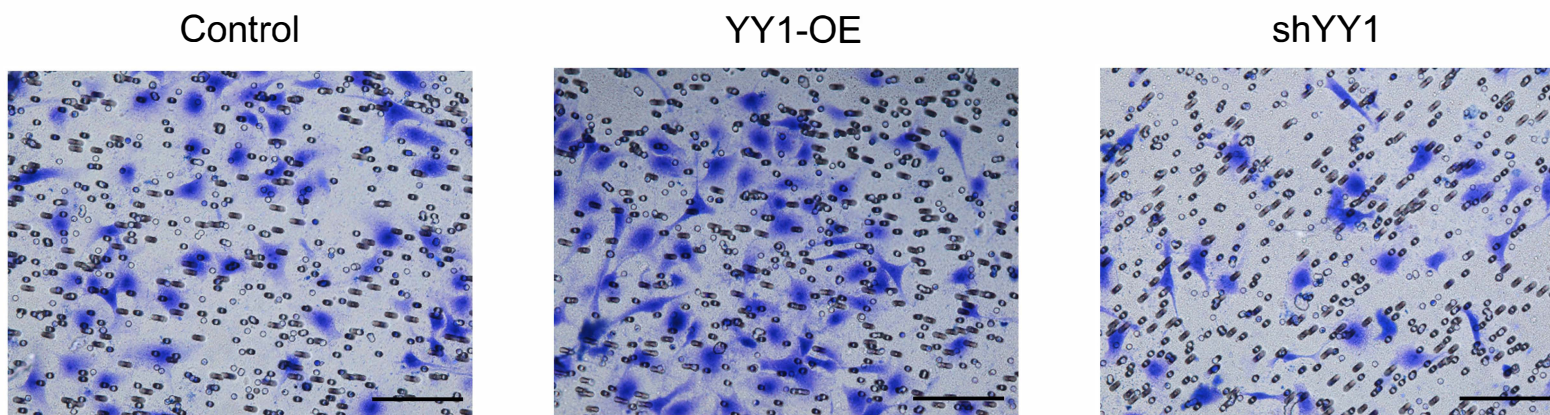
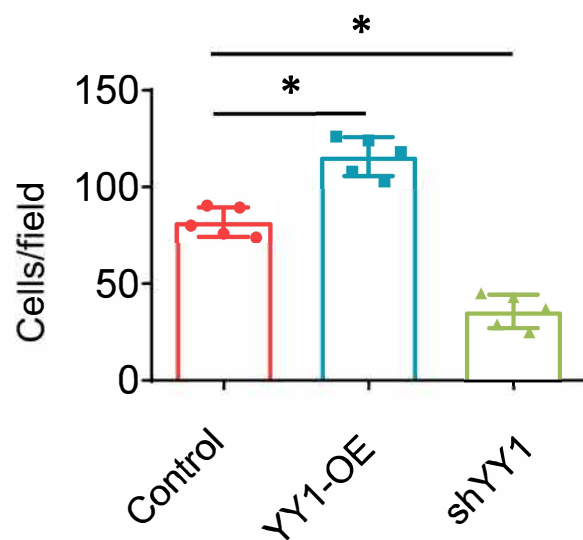




**Figure S1. YY1 inhibited cardiomyocyte apoptosis and caspase 3 cleavage.**

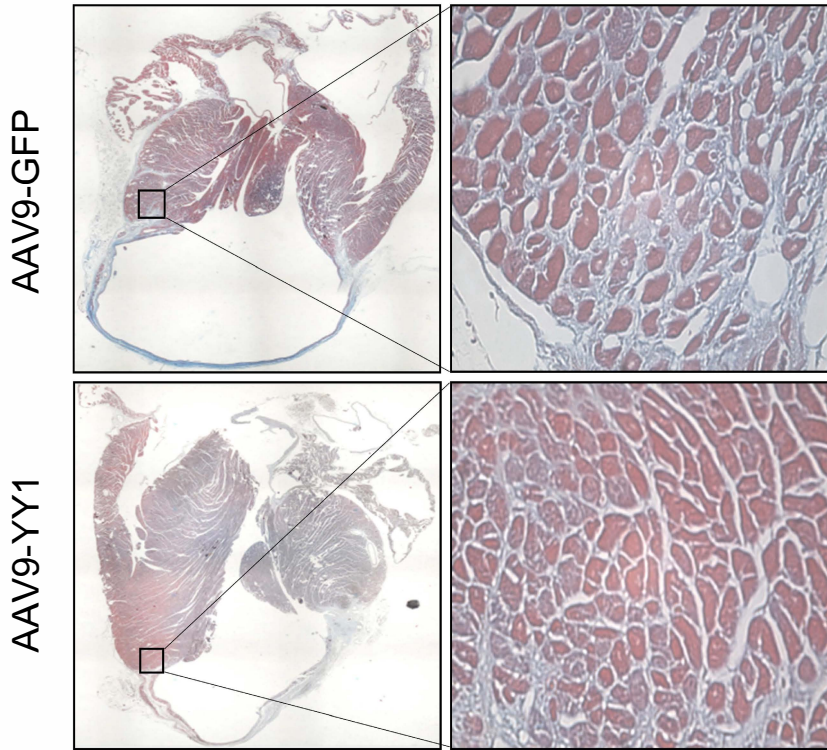
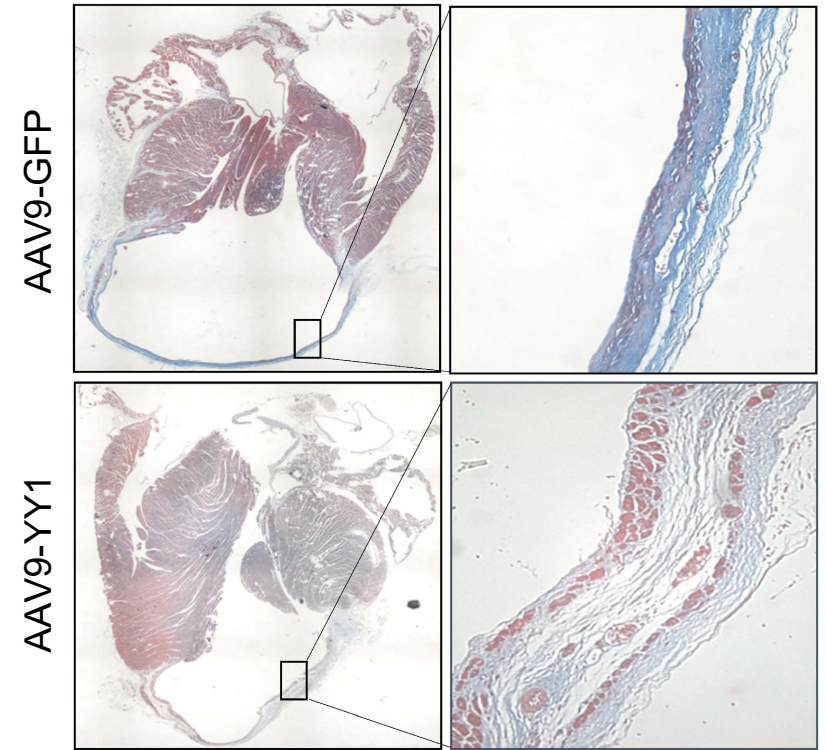
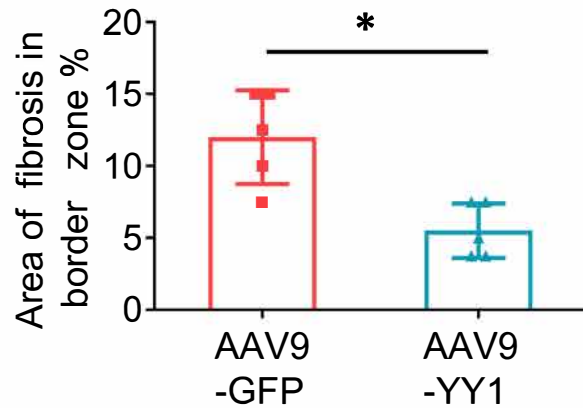
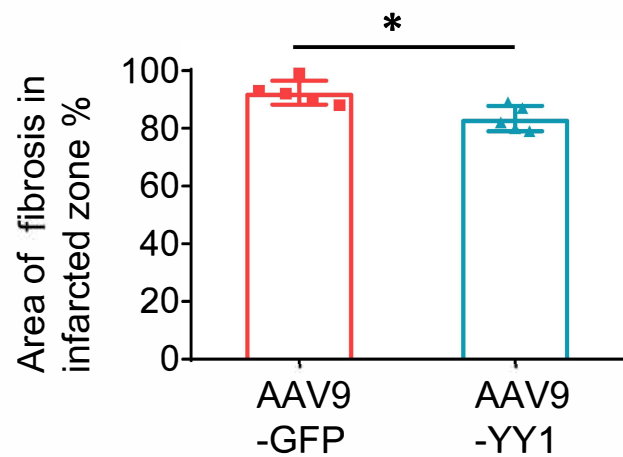
**A and B:** The representative image (A) and statistical result (B) of TUNEL positive NRVMs with or without YY1 over-expression and hypoxia treatment (1% O<sub>2</sub> for 24 hours), \*P < 0.05, n=6, scale bar=50μm.

**C and D:** The representative image (C) and statistical result (D) of the cleaved-caspase3 protein levels in NRVMs with or without YY1 over-expression and hypoxia treatment (1% O<sub>2</sub> for 24 hours), \*P < 0.05, n=6. YY1-OE stands for YY1 over-expression. cTnI stands for cardiac troponin I.

**A****B**

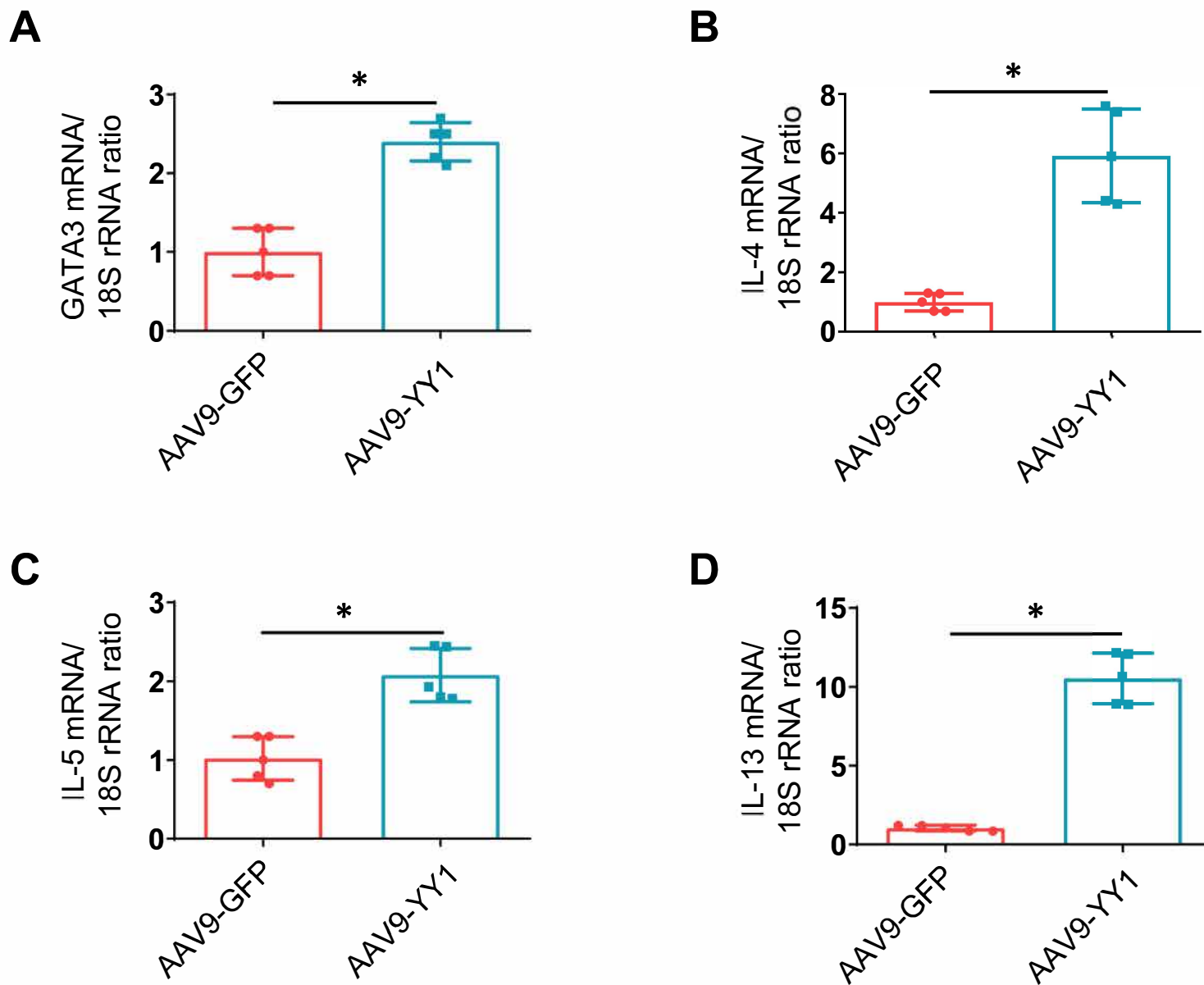
**Figure S2. YY1 increased HUVECs migration in transwell assay.**

**A and B:** The representative image (A) and statistical result (B) of crystal violet staining of migrated HUVECs transfected with YY1 over-expression (YY1-OE) or YY1 silencing (shYY1) plasmids. \*P< 0.05, n=5, scale bar = 50 $\mu$ m.

**A1****B1****A2****B2**

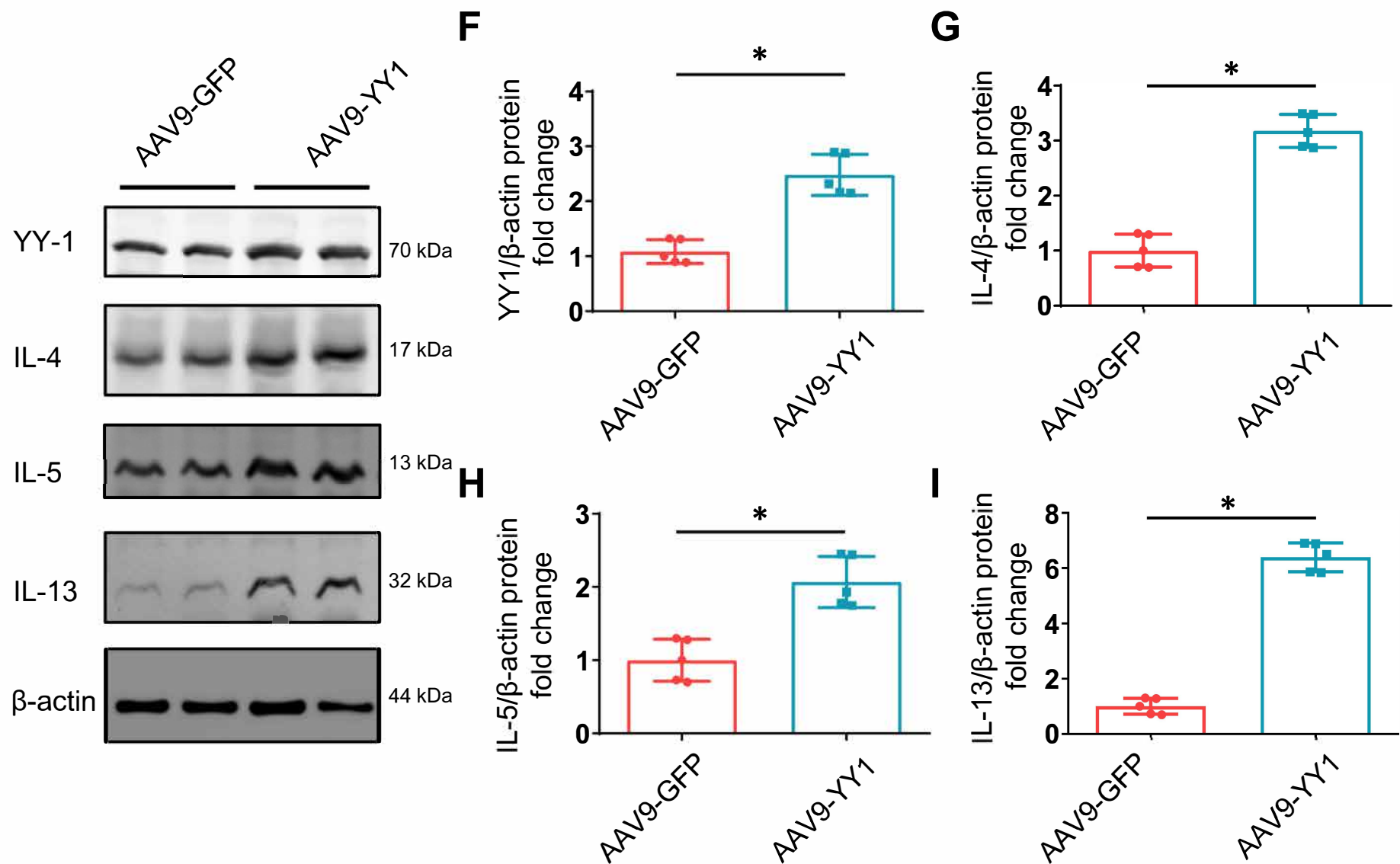
### Figure S3. YY1 limited the cardiac fibrosis post MI.

**A** and **B**: The percent of fibrosis area examined by Masson's trichrome staining in the infarcted border zone (A1 and A2) and the infarcted region (B1 and B2) of mouse heart 4 weeks post MI in AAV9-YY1 group and AAV9-GFP group, black square and lines in the representative image indicated the magnification (right panels) of the selected area in left panels, \* $P < 0.05$ ,  $n = 5$ .

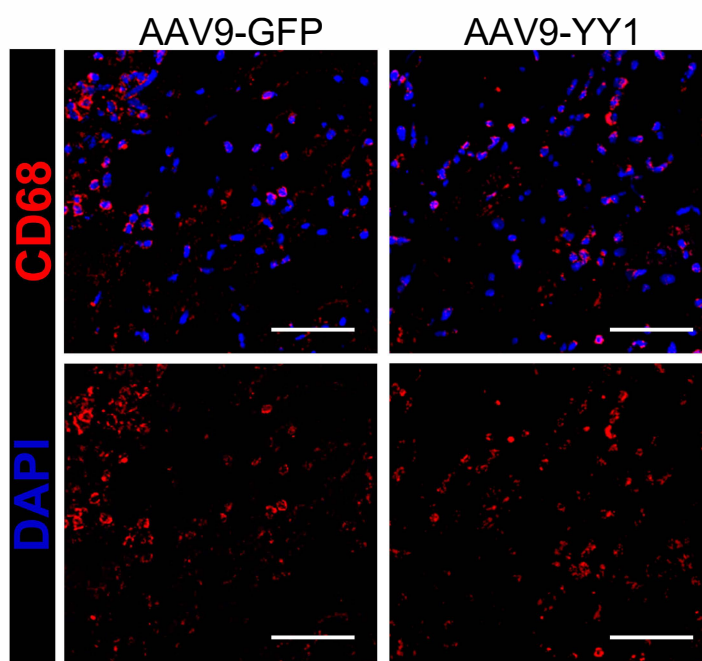
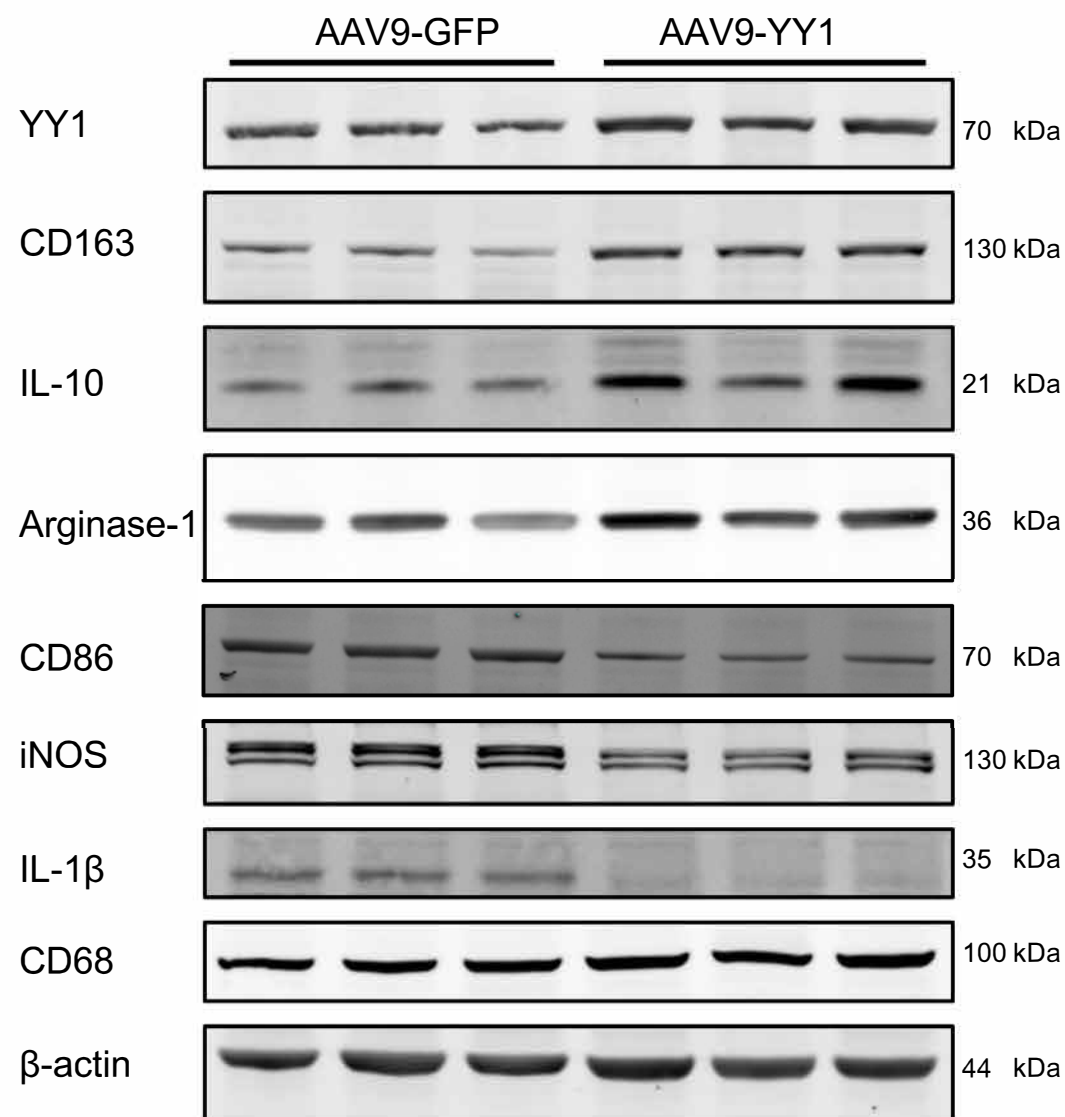
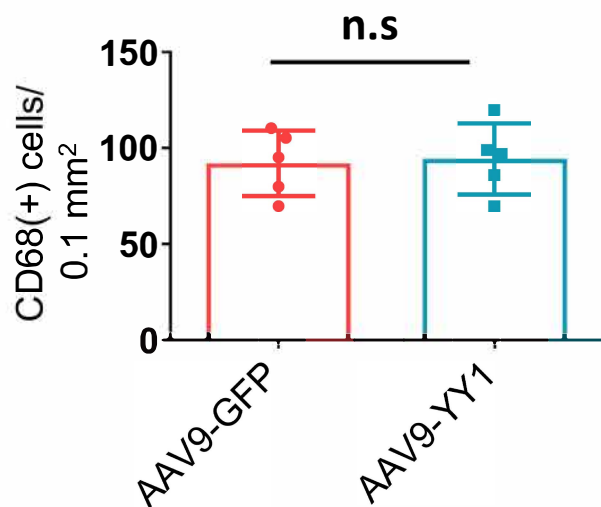


**Figure S4. YY1 up-regulated Th2 cytokine production in post-MI mouse heart.**

**A-D:** The mRNA levels of GATA3 (A), IL-4(B), IL-5 (C), IL-13 (D) in mouse heart 5 days post MI in AAV9-YY1 and AAV9-GFP groups, \*P<0.05, n=5.

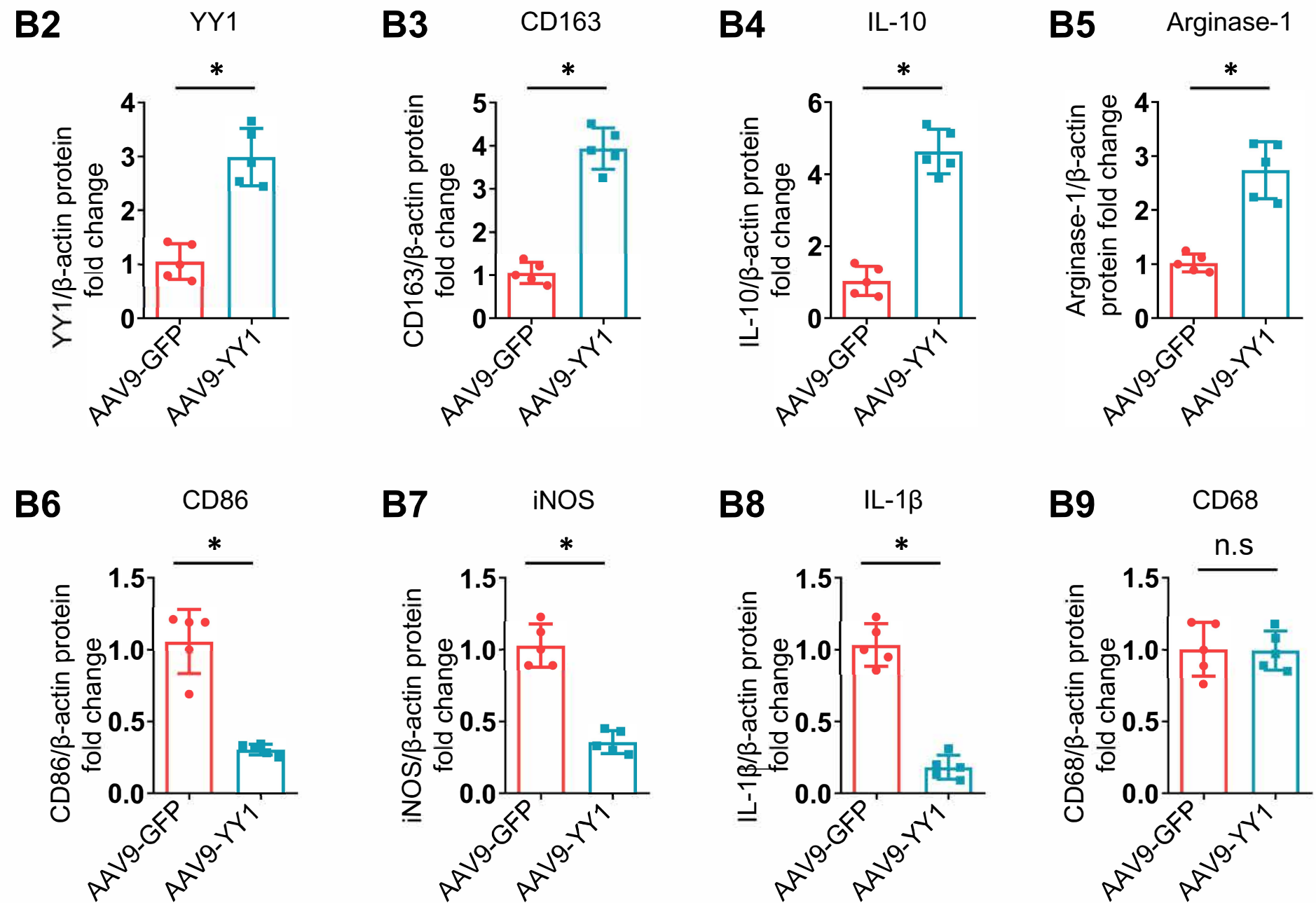


**E-I:** The representative image (E) of western blot and statistical results of YY1 (F), IL-4 (G), IL-5 (H) and IL-13 (I) in mouse heart 5 days post MI in AAV9-YY1 and AAV9-GFP groups, \* $P < 0.05$ ,  $n = 5$ .

**A1****B1****A2**

**Figure S5. YY1 promoted M2 macrophage polarization in post-MI mouse heart.**

**A1** and **A2**: The representative image (**A1**) and statistical results of the CD68(+) macrophage infiltration in border zone of mouse heart 5 days post MI in AAV9-YY1 and AAV9-GFP groups, n.s: non-significant, n=5, scale bar=50μm. **B1**: The representative image of western blot of YY1 , CD163, IL-10, Arginase-1, CD86, iNOS , IL-1β, and CD68 in mouse heart 5 days post MI in AAV9-YY1 and AAV9-GFP groups, \*P<0.05, n.s: non-significant, n=5.



**B2-B9:** The statistical results of western blot for YY1 (B2), CD163 (B3), IL-10 (B4), Arginase-1 (B5), CD86 (B6), iNOS (B7), IL-1 $\beta$  (B8), and CD68 (B9) in mouse heart 5 days post MI in AAV9-YY1 and AAV9-GFP groups, \*P<0.05, n.s: non-significant, n=5.